10 Nash RA, Pepe MS, Storb R *et al.* Acute graft-versus-host disease: analysis of risk factors after allogeneic marrow transplantation and prophylaxis with cyclosporine and methotrexate. *Blood* 1992; **80**: 1838–1845.
11 Atkinson K, Horowitz MM, Gale RP *et al.* Risk factors for chronic graft-versus-host disease after HLA-identical sibling bone marrow transplantation. *Blood* 1990; **75**: 2459–2464.
12 Carlens S, Ringden O, Remberger M *et al.* Risk factors for chronic graft-versus-host disease after bone marrow transplantation: a retrospective single centre analysis. *Bone Marrow Transplant* 1998; **22**: 755–761.
13 Ringden O, Horowitz MM, Gale RP *et al.* Outcome after allogeneic bone marrow transplant for leukemia in older adults. *JAMA* 1993; **270**: 57–60.
14 Cahn JY, Labopin M, Schattenberg A *et al.* Allogeneic bone marrow transplantation for acute leukemia in patients over the age of 40 years. Acute Leukemia Working Party of the European Group for Bone Marrow Transplantation (EBMT). *Leukemia* 1997; **11**: 416–419.
15 Hartman AR, Williams SF, Dillon JJ. Survival, disease-free survival and adverse effects of conditioning for allogeneic bone marrow transplantation with busulfan/cyclophosphamide *vs* total body irradiation: a meta-analysis. *Bone Marrow Transplant* 1998; **22**: 439–443.
16 Socie G, Clift RA, Blaise D *et al.* Busulfan plus cyclophosphamide compared with total-body irradiation plus cyclophosphamide before marrow transplantation for myeloid leukemia: long-term follow-up of 4 randomized studies. *Blood* 2001; **98**: 3569–3574.
17 Blaise D, Maraninchi D, Archimbaud E *et al.* Allogeneic bone marrow transplantation for acute myeloid leukemia in first remission: a randomized trial of a busulfan-Cytoxan *versus* Cytoxan-total body irradiation as preparative regimen: a report from the Group d'Etudes de la Greffe de Moelle Osseuse. *Blood* 1992; **79**: 2578–2582.
18 Ringden O, Ruutu T, Remberger M *et al.* A randomized trial comparing busulfan with total body irradiation as conditioning in allogeneic marrow transplant recipients with leukemia: a report from the Nordic Bone Marrow Transplantation Group. *Blood* 1994; **83**: 2723–2730.
19 Blume KG, Kopecky KJ, Henslee-Downey JP *et al.* A prospective randomized comparison of total body irradiation-etoposide *versus* busulfan-cyclophosphamide as preparatory regimens for bone marrow transplantation in patients with leukemia who were not in first remission: a Southwest Oncology Group study. *Blood* 1993; **81**: 2187–2193.
20 Clift RA, Buckner CD, Thomas ED *et al.* Marrow transplantation for chronic myeloid leukemia: a randomized study comparing cyclophosphamide and total body irradiation with busulfan and cyclophosphamide. *Blood* 1994; **84**: 2036–2043.
21 Devergie A, Blaise D, Attal M *et al.* Allogeneic bone marrow transplantation for chronic myeloid leukemia in first chronic phase: a randomized trial of busulfan-cytoxan *versus* cytoxan-total body irradiation as preparative regimen: a report from the French Society of Bone Marrow Graft (SFGM). *Blood* 1995; **85**: 2263–2268.

International Journal of
HEMATOLOGY

Efficacy and Safety of Imatinib Mesylate for Patients in the First Chronic Phase of Chronic Myeloid Leukemia: Results of a Japanese Phase II Clinical Study

Yasuo Morishima,[a] Michinori Ogura,[a] Miki Nishimura,[b] Fumiharu Yazaki,[c] Masami Bessho,[c] Hideaki Mizoguchi,[d] Shigeru Chiba,[e] Hisamaru Hirai,[e] Tetsuzo Tauchi,[f] Akio Urabe,[g] Masatomo Takahashi,[h] Kazunori Ohnishi,[i] Toshiya Yokozawa,[j] Nobuhiko Emi,[j] Masami Hirano,[k] Chihiro Shimazaki,[l] Shinji Nakao,[m] Yasukazu Kawai,[n] Masahiro Fujimoto,[o] Hirokuni Taguchi,[p] Itsuro Jinnai,[q] Ryuzo Ohno[r]

[a]Department of Hematology and Cell Therapy, Aichi Cancer Center Hospital, Nagoya; [b]Second Department of Internal Medicine, Chiba University School of Medicine, Chiba; [c]Department of Hematology, Saitama Medical School, Saitama; [d]Department of Hematology, Tokyo Women's Medical University School of Medicine, Tokyo; [e]Department of Hematology/Oncology and Cell Therapy/Transplantation Medicine, University of Tokyo Hospital, Tokyo; [f]First Department of Internal Medicine, Tokyo Medical University, Tokyo; [g]Department of Hematology, NTT Kanto Medical Center, Tokyo; [h]Division of Hematology and Oncology, St. Marianna University School of Medicine, Kawasaki; [i]Third Department of Internal Medicine, Hamamatsu University School of Medicine, Hamamatsu; [j]Department of Hematology, Nagoya University Graduate School of Medicine, Nagoya; [k]Department of Medicine, Fujita Health University School of Medicine, Toyoake; [l]Second Department of Medicine, Kyoto Prefectural University of Medicine, Kyoto; [m]Cellular Transplantation Biology, Kanazawa University Graduate School of Medical Science, Kanazawa; [n]First Department of Internal Medicine, Faculty of Medical Sciences, University of Fukui, Fukui; [o]First Department of Internal Medicine, Kansai Medical University, Osaka; [p]Department of Hematology and Respiratory Medicine, Kochi Medical School, Kochi University, Kochi; [q]Department of Hematology, Atomic Bomb Disease Institute, Nagasaki University Graduate School of Biosciences, Nagasaki; [r]Aichi Cancer Center, Nagoya, Japan

Received April 27, 2004; received in revised form June 4, 2004; accepted June 7, 2004

Abstract

Imatinib mesylate is a relatively new drug that targets the BCR-ABL chimeric protein, the molecular basis of chronic myeloid leukemia (CML). A phase II clinical trial in 39 Japanese patients in the first chronic phase of CML was conducted with imatinib mesylate at a dose of 400 mg/day. Hematologic complete response was obtained in 92.3% of the patients, complete cytogenetic response (CR) was obtained in 43.6%, and major partial CR was obtained in 20.5% of the patients. Although 29 of 39 patients required an adjustment of dosing because of grade 3 or 4 adverse events, most of the events were reversible, and 25 of the 29 patients were able to resume therapy. Between day 15 and day 35, grade 3 or 4 neutropenia and/or leukocytopenia occurred in 13 patients, and grade 3 thrombocytopenia occurred in 5 patients. Overall, nonhematologic grade 3 adverse events occurred in 28.2% of the patients. These data support the use of imatinib mesylate as the treatment of choice for chronic-phase CML patients.
Int J Hematol. 2004;80:261-266. doi: 10.1532/IJH97.04074

Key words: Imatinib mesylate; Chronic myeloid leukemia; Phase II clinical study

1. Introduction

Chronic myeloid leukemia (CML) is a hematologic disease arising from the malignant transformation of hematopoietic stem cells and is characterized by the excessive proliferation of myeloid cells. The characteristic feature of CML is the presence of the Philadelphia chromosome (Ph) in hematopoietic cells, which is caused by the reciprocal translocation of t(9;22) [1-3]. The fused transcripts of the *abl* and *bcr* genes produce the chimeric BCR-ABL protein, a constitutively active tyrosine kinase [4].

The clinical course of CML consists of 3 phases. The chronic phase is a period of proliferation and differentiation of myeloid cells. After several years, the chronic phase proceeds to the accelerated phase and terminates in blast crisis.

Correspondence and reprint requests: Morishima Yasuo, MD, Department of Hematology and Cell Therapy, Aichi Cancer Center Hospital, 1-1 Kanokoden Chikusa-ku, Nagoya, Japan 464-8681; 052-762-6111; fax: 052-764-2923 (e-mail: ymorisim@aichi-cc.jp).

which is characterized by the transformation of the hematopoietic cells to acute blast cells with a clinical picture similar to that of acute leukemias.

Considerable progress has been made in the therapy of CML over the past 20 years. Interferon α (IFN-α) has been shown to reduce or diminish Ph^- malignant cells and prolong the duration of the chronic phase [5,6]. Allogeneic hematopoietic stem cell transplantation (HSCT) has been established as the only mode of curative therapy, especially for patients in the chronic phase of CML, and more than two thirds of chronic-phase patients who receive an HSCT from an HLA-matched sibling or unrelated donor can be considered cured of the disease [7,8].

In the 1990s, a promising new drug, imatinib mesylate (Gleevec; Novartis Pharmaceuticals, East Hanover, NJ, USA), targeting the BCR-ABL chimeric protein [9,10] was developed. This potent competitive inhibitor of BCR-ABL tyrosine kinase activity specifically blocks proliferation and promotes the in vitro apoptosis of cells containing this protein.

Two clinical phase I studies were first conducted. One was carried out for patients with chronic-phase CML [11], and the other was for patients with blast crisis CML and acute lymphoblastic leukemia [12]. These studies were followed by a large-scale international phase II study for IFN-resistant patients with chronic-phase CML [13]. A clinical phase I study for Japanese patients was also conducted for IFN-resistant patients with chronic-phase CML (unpublished data).

The analysis of these clinical trials clearly demonstrated that (1) the drug-related adverse events of imatinib mesylate were minimal and clinically acceptable and (2) the response to imatinib mesylate was remarkable. Kantarjian et al reported that 60% of IFN-resistant patients achieved a major cytogenetic response (CR) and that 95% showed a complete hematologic response (HR) [13].

In the present study, a phase II clinical trial of imatinib mesylate was conducted at a dose of 400 mg/day in Japanese patients with chronic-phase CML. Primary end points were HR and the safety of imatinib mesylate, and secondary end points were the duration of HR and the rate of CR.

2. Patients and Methods

2.1. Patient Eligibility Criteria

Patients with chronic-phase CML fulfilling the following criteria were enrolled in this phase II study. Patient age ranged from 15 years to 74 years. Patients were classified into 1 of the following 4 treatment categories: (1) no HR, consisting of patients who failed to achieve complete HR with the administration of IFN for more than 3 months or who failed to maintain a complete HR by IFN therapy; (2) no CR, consisting of patients who showed more than 65% Ph^+ cells in the bone marrow with the administration of IFN for more than 1 year or who showed a 1-month increase of Ph^+ cells of greater than 30% in the bone marrow despite IFN administration; (3) IFN-intolerant patients who stopped receiving IFN because of adverse events caused by IFN; and (4) patients with no history of IFN therapy.

Exclusion criteria included the following characteristics: (1) fewer than 10,000/μL white blood cells in the peripheral blood; (2) a serum bilirubin or creatinine level elevated more than 2-fold higher than the upper limit of the normal value; (3) a serum glutamic-oxaloacetic transaminase or glutamic-pyruvic transaminase level elevated more than 3-fold higher than the upper limit of the normal value; (4) eligibility for allogeneic HSCT from an HLA-identical sibling or unrelated donor; (5) a history of HSCT; (6) cardiac disease of more than grade 3 according to the New York Heart Association scale; and (7) a history of administration of busulfan within the previous 6 weeks, IFN-α within 2 weeks, cytosine arabinoside within 2 weeks, or hydroxyurea within 1 week.

Each patient signed an informed consent form at the time of study entry. The study was approved by the institutional review board of each institution.

2.2. Study Design and Treatment Schedule

The study was designed by the investigators and representatives of the sponsor, Novartis Pharmaceuticals. The data were collected and analyzed with the use of the data-management and statistical support of Novartis Pharmaceuticals in close collaboration with the investigators.

A 400-mg dose of imatinib mesylate was administered orally once a day 2 hours after breakfast for 12 weeks. Optional continuation of imatinib mesylate administration was scheduled thereafter.

When an adverse event occurred, the dosage was adjusted according to the following rules. When a grade 3 or 4 leukocyte (neutrophil) or platelet adverse event was observed, imatinib mesylate was discontinued until cell counts recovered to grade 2 or less. When a grade 2 or greater nonhematologic adverse event was observed, imatinib mesylate was discontinued until the patient improved to grade 1, and then it was readministered at the same dose in cases of a grade 2 event and at a 100-mg reduced dose in cases of a grade 3 event.

2.3. Assessment of Tumor Response and Toxicity

Tumor response was determined according to the following response criteria. A complete HR was defined as reduction of the leukocyte count to less than 10,000/μL and the platelet count to less than 500,000/μL for at least 4 weeks. CR was determined by the percentage of Ph^+ cells in the bone marrow. From the chromosomal analysis of 20 cells in metaphase, CR was further categorized as complete CR (no Ph^+ cells), major partial CR (1%-35% Ph^+ cells), minor partial CR (36%-65% Ph^+ cells), minimal partial response (66%-95% Ph^+ cells), and no response (96%-100% Ph^+ cells). When chromosomal analysis was not available, the results of fluorescent in situ hybridization analysis were substituted, and finding less than 1.3% Ph^+ cells in a fluorescent in situ hybridization analysis was regarded as a complete CR.

Adverse events were graded according to National Cancer Institute Common Toxicity Criteria version 2.0, and the cumulative tumor response rate was calculated by the Kaplan-Meier method.

Table 1.
Patient Characteristics*

	Prior Interferon Therapy Status				
	No Hematologic Response (n = 7)	No Cytogenetic Response (n = 15)	Interferon Intolerant (n = 10)	No Interferon Therapy (n = 7)	Total (N = 39)
Age, y	52 (32-71)	56 (26-66)	58 (23-69)	55 (35-71)	56 (23-71)
Body weight, kg	65.0 (45.0-77.0)	61.0 (49.0-86.0)	61.5 (42.7-79.0)	63.5 (44.3-75.3)	62.0 (42.7-86.0)
Male/female sex, n	4/3	10/5	6/4	4/3	24/15
Performance status (grade 0/1), n	7/0	13/2	10/0	7/0	37/2
Duration from diagnosis, n					
≤6 mo			1	2	3
6-12 mo	2		2	3	7
12-24 mo		6	2		8
24-60 mo	2	5	1	1	9
>60 mo	3	4	4	1	12
Duration of interferon therapy, n					
No therapy				7	7
≤6 mo			4		4
6-12 mo	2		1		3
12-24 mo	1	8	2		11
24-60 mo	2	5	2		9
>60 mo	2	2	1		5
WBC count before imatinib treatment, $\times 10^4/\mu L$	2.44 (1.447-5.37)	1.30 (0.94-3.15)	2.21 (1.045-9.1)	1.43 (1.2-9.42)	1.45 (0.94-9.42)
Platelet count before imatinib treatment, $\times 10^4/\mu L$	35.2 (14.1-168.3)	27.8 (8.1-143.0)	30.7 (17.6-67.8)	30.25 (27.7-66.6)	30.35 (8.1-168.3)
Splenomegaly (>10 cm below the costal margin)	0	0	0	0	0

*Data are presented as the median (range) where appropriate. WBC indicates white blood cell.

3. Results

3.1. Patients and Treatment

Forty-three patients were enrolled between January 22, 2001, and May 10, 2001. Four patients were excluded because of low white blood cell counts (fewer than 10,000/μL just before scheduled administration) according to the protocol, so that 39 patients were evaluable for safety and response. The characteristics of these patients are summarized in Table 1. Twenty-two patients had a history of no response to prior IFN therapy, 10 were intolerant to prior IFN treatment, and 7 had undergone no prior IFN therapy at the time of registration. Patient ages ranged from 23 to 71 years (median, 56 years). Twenty-four patients were male, and 15 were female.

The duration of imatinib mesylate administration ranged from 11 to 292 days (median, 237 days). The dosage was adjusted for 32 patients because of adverse effects (30 patients), no tumor effect (1 patient), or both (1 patient). Of these 32 patients, drug administration was stopped in 29 patients, transiently in 27 patients and permanently in 2 patients. The dosage of imatinib mesylate was increased in 2 patients because of insufficient tumor response.

Bone marrow aspiration was performed every 3 months for the assessment of CRs, and clinical responses, including any adverse events of imatinib mesylate, were observed for a median of 270 days (range, 15-300 days) after the initial administration.

3.2. Response Rate

Complete HR was obtained in 36 (92.3%) of 39 patients and required 6 to 56 days (median, 15 days) of treatment to achieve (Figure 1; Table 2). Two patients who did not obtain HR or CR showed disease progression to blast crisis on day 168 and day 248 after the administration of 400 mg/day. One patient received a subtherapeutic dose of imatinib mesylate because of the adverse effect of thrombocytopenia and showed no HR.

CR was assessed every 3 months, and the cumulative duration to achieve complete CR and major partial CR is

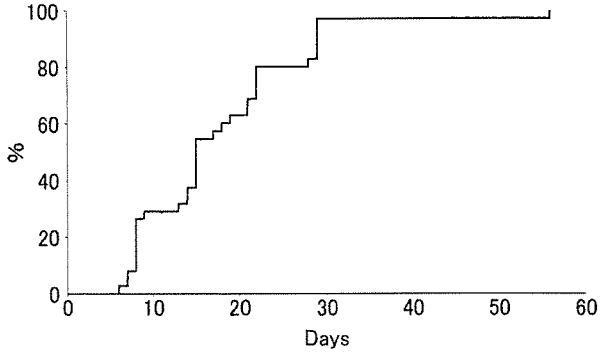

Figure 1. Cumulative days to achieve complete hematologic response (HR) after the administration of imatinib mesylate in patients with HR.

Table 2.
Response Rate of Imatinib Mesylate in Patients with Chronic-Phase Chronic Myeloid Leukemia

	Prior Interferon Therapy Status				
	No Hematologic Response (n = 7), n	No Cytogenetic Response (n = 15), n	Interferon Intolerant (n = 10), n	No Interferon Therapy (n = 7), n	Total (N = 39), n (%)
Hematologic response					
Complete remission	7	13	9	7	36 (92.3)
Not evaluable	0	2	1	0	3
Cytogenetic response					
Complete	3	8	3	3	17 (43.6)
Major partial	2	2	2	2	8 (20.5)
Minor partial	0	1	0	0	1 (2.6)
Minimal partial	0	0	2	1	3 (7.7)
No response	2	3	2	1	8 (20.5)
Not evaluable	0	1	1	0	2 (5.1)

shown in Figure 2. By 3 months after the start of therapy, 21% and 46% of patients achieved complete CR and major partial CR, respectively. The cumulative incidence of complete CR increased to 41% at 6 months and reached 44% during the clinical study period. There were no differences in CR rate according to prior IFN treatment status between the 4 groups.

3.3. Adverse Events

Hematologic adverse events were observed in 23 of 39 patients (Table 3). Neutropenia of grade 3 or 4 occurred in 14 patients, and thrombocytopenia of grade 3 or 4 occurred in 12 patients. Neutropenia appeared within 22 to 103 days (median, 46 days) after the administration of imatinib mesylate, and thrombocytopenia appeared within 15 to 197 days (median, 35 days).

Nonhematologic adverse events were observed in 36 patients (Table 3). Grade 3 and grade 1 to 2 skin rash occurred in 7 patients (17.9%) and 11 patients (28.2%), respectively. Grade 3 vomiting occurred in 2 patients (5.1%), and grade 3 myalgia occurred in 1 patient (2.6%). Other frequent grade 1 to 2 adverse events were nausea (43.6%), diarrhea (20.5%), fatigue (20.5%), edema of the eyelid (33.3%) or face (15.4%), muscle cramps (15.4%), taste disturbance (12.8%), and arthralgia (10.3%).

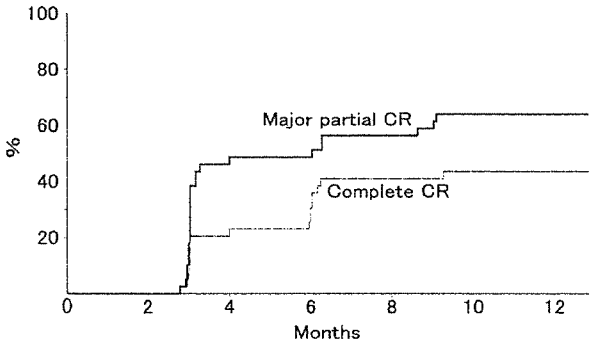

Figure 2. Cumulative incidence of major partial cytogenetic response (CR).

Liver dysfunction was observed in 2 patients (grade 2 and grade 3), and elevation of the serum alkaline phosphatase level (greater than grade 3) with no clinical signs and symptoms was noted in 10 patients.

Serious drug-related adverse events were reported in 9 patients. Neutropenia occurred in 6 patients, thrombocytopenia in 1, neutropenia and thrombocytopenia in 1, and herpes zoster in 1.

Only 2 patients permanently discontinued imatinib mesylate treatment, 1 patient at day 12 because of myalgia and the other because of recurrent grade 3 neutropenia. Of the other 29 patients who required dose adjustment or interruption, all patients resumed therapy again at 400 mg/day or with a decreased dose after they recovered from the adverse events.

3.4. Patient Survival

During the observation period, only 1 of the 39 patients died from progression of the disease into blast crisis.

4. Discussion

Imatinib mesylate has demonstrated excellent antileukemia effects in this Japanese phase II study of CML patients in the chronic phase, most of whom were IFN resistant or intolerant.

This phase II study was designed as part of a phase I/II study of imatinib mesylate for treating chronic-phase CML, and the dose was determined according to the data of the preceding dose-finding phase I study conducted with doses of 200, 400, and 600 mg/day of imatinib mesylate. The data from the phase I part of the study indicated that 600 mg/day was tolerable; however, 200 mg/day was not sufficient for the achievement of a CR (unpublished data). Thus, the phase II study was conducted at an imatinib mesylate dose of 400 mg/day for 8 weeks.

Complete HR was obtained in 92.3% of the patients, complete CR was obtained in 43.6%, and minor partial CR was obtained in 20.5% (Table 2). These response rates were comparable with those of a large-scale international phase II study using the same single dose of 400 mg/day in IFN-resistant patients in the chronic phase [13].

Table 3.
Adverse Events Related to Treatment with Imatinib Mesylate

Event	No. of Patients with Event, n (%)		
	Grades 1-4	Grade 3	Grade 4
Nonhematologic	36 (92.3)	11 (28.2)	0
Skin and subcutaneous tissue disorders			
Dermatitis	18 (46.2)	7 (17.9)	0
Eyelid edema	13 (33.3)	0	0
Face edema	6 (15.4)	0	0
Gastrointestinal disorders			
Nausea	17 (43.6)	0	0
Diarrhea	8 (20.5)	0	0
Vomiting	6 (15.4)	2 (5.1)	0
Abdominal pain	4 (10.3)	0	0
General disorders			
Fatigue	8 (20.5)	0	0
Edema	6 (15.4)	0	0
Muscle-skeletal, connective tissue, and bone disorders			
Muscle cramps	6 (15.4)	0	0
Arthralgia	4 (10.3)	0	0
Myalgia	4 (10.3)	1 (2.6)	0
Nervous system disorders			
Taste disturbance	5 (12.8)	0	0
Hematologic	24 (61.5)	21 (53.8)	7 (17.9)
Thrombocytopenia	15 (38.5)	11 (28.2)	1 (2.6)
Neutropenia	14 (35.9)	8 (20.5)	6 (15.4)
Leukopenia	13 (33.3)	10 (25.6)	2 (5.1)
Anemia	6 (15.4)	2 (5.1)	1 (2.6)

Although the patient body surface area (median, 1.68 m^2; range, 1.27-2.05 m^2) in this Japanese study cohort was smaller than that reported for non-Japanese studies, the frequency and grade of adverse events were similar. The serum concentrations of imatinib mesylate determined in the pharmacologic study of the phase I part of this Japanese study were not significantly different from those of an international phase I study. These results indicate that a dose of 400 mg/day is an appropriate initial dose of imatinib mesylate in adult CML patients in the chronic phase.

We consider it important to understand the time until response and the duration of response to imatinib mesylate, because alternative treatments, such as allogeneic HSCT from HLA-identical related or unrelated donors, could be one of the choices for imatinib mesylate–resistant patients. Our data indicate that administration for at least 6 months is necessary to achieve complete CR or major partial CR. When a patient is a poor responder (that is, he or she shows no response or minor partial CR after 3 or 6 months of administration), an increase of the dosage to more than 600 mg may be another choice for treatment. Kantarjian et al recently reported the efficacy and safety of 800 mg/day in treating CML in the chronic phase [14].

To predict the efficacy of imatinib mesylate for individual patients, Kaneta et al analyzed the expression profiles of CML cells from the 18 CML patients who were treated in this phase II study [15]. The analysis of complementary DNA microarrays representing 23,040 genes identified 79 genes that were expressed differentially between responders and nonresponders to imatinib mesylate. Validation of these findings is ongoing in another cohort of patients. Thus, these results may provide the first evidence that gene expression profiling can be used to predict the sensitivity of CML cells to imatinib mesylate.

Although 29 of the 39 patients had their imatinib mesylate dosing interrupted according to the dose-adjustment rules in the protocol because of adverse events, most of the events were reversible, and 25 patients resumed treatment. Between days 15 and 35, neutropenia and/or leukopenia of grade 3 or 4 occurred in 13 patients, and grade 3 thrombocytopenia occurred in 5 patients. We suspect that during this period, Ph^+ hematopoietic cells decreased or disappeared in the bone marrow in responsive patients and that normal hematopoiesis had not yet fully recovered. Therefore, close attention should be paid during this period to monitoring for the occurrence of these specific adverse hematologic events. The administration of granulocyte colony-stimulating factor might also be considered when severe neutropenia and neutropenic fever become evident [16].

Recently, a large-scale international randomized phase III clinical study in patients with newly diagnosed chronic-phase CML that compared imatinib mesylate with the combination of IFN and cytosine arabinoside clearly indicated that imatinib mesylate was more effective as first-line therapy for patients with chronic-phase CML [17]. Furthermore, Kantarjian et al reported a follow-up analysis of the phase II study in treating chronic-phase CML that showed that imatinib mesylate maintained favorable outcomes in chronic-phase CML after a median duration of therapy of 29 months [18]. However, because of reports that patients who did not achieve a CR with imatinib mesylate had significantly worse survival times than responding patients, we can recommend

that when such patients are identified, they should be immediately considered for alternative treatments [19].

Thus, the results of this study provide additional and corroborative evidence for using imatinib mesylate as the treatment of choice for chronic-phase CML patients.

Follow-up for more than 5 years will be required to evaluate the long-term safety and tolerance of this drug, the durability of responses, and the potential for cure, as well as to identify the situations in which alternative therapy can be recommended.

References

1. Rowley JD. A new consistent chromosomal abnormality in chronic myelogenous leukaemia identified by quinacrine fluorescence and Giemsa staining. *Nature*. 1973;243:290-293.
2. Groffen J, Stephenson JR, Heisterkamp N, de Klein A, Bartram CR, Grosveld G. Philadelphia chromosomal breakpoints are clustered within a limited region, *bcr*, on chromosome 22. *Cell*. 1984;36:93-99.
3. Sattler M, Griffin JD. Mechanisms of transformation by BCR/ABL oncogene. *Int J Hematol*. 2001;73:278-291.
4. Shtivelman E, Lifshitz B, Gale RP, Canaani E. Fused transcript of *abl* and *bcr* genes in chronic myelogenous leukemia. *Nature*. 1985; 315:550-554.
5. Chronic Myeloid Leukemia Trialists' Collaborative Group. Interferon alfa versus chemotherapy for chronic myeloid leukemia: a meta-analysis of seven randomized trials. *J Natl Cancer Inst*. 1997; 89:1616-1620.
6. Ohnishi K, Ohno R, Tomonaga M, et al. A randomized trial comparing interferon-α with busulfan for newly diagnosed chronic myelogenous leukemia in chronic phase. *Blood*. 1995;86:906-916.
7. Hansen JA, Gooley T, Martin PJ, et al. Bone marrow transplants from unrelated donors for patients with chronic myeloid leukemia. *N Engl J Med*. 1998;338:962-968.
8. Kodera Y, Morishima Y, Kato S, et al. Analysis of 500 bone marrow transplants from unrelated donors (UR-BMT) facilitated by the Japan Marrow Donor Program: confirmation of UR-BMT as a standard therapy for patients with leukemia and aplastic anemia. *Bone Marrow Transplant*. 1999;24:995-1003.
9. Druker BJ, Tamura S, Buchdunger E, et al. Effects of a selective inhibitor of the Abl tyrosine kinase on growth of Bcr-Abl positive cells. *Nat Med*. 1996;2:561-560.
10. Carroll M, Ohno-Jones S, Tamura S, et al. CGP 57148, a tyrosine kinase inhibitor, inhibits the growth of cells expressing BCR-ABL, TEL-ABL, and TEL-PDGFR fusion proteins. *Blood*. 1997;90: 4947-4952.
11. Druker BJ, Talpatz M, Resta DJ, et al. Efficacy and safety of a specific inhibitor of the BCR-ABL tyrosine kinase in chronic myeloid leukemia. *N Engl J Med*. 2001;344:1031-1037.
12. Druker BJ, Sawyers CL, Kantarjian H, et al. Activity of a specific inhibitor of the BCR-ABL tyrosine kinase in the blast crisis of chronic myeloid leukemia and acute lymphoblastic leukemia with the Philadelphia chromosome. *N Engl J Med*. 2001;344:1038-1042.
13. Kantarjian H, Sawyer C, Hochhaus A, et al. Hematologic and cytogenetic responses to imatinib mesylate in chronic myelogenous leukemia. *N Engl J Med*. 2002;346:645-652.
14. Kantarjian H, Talpaz M, O'Brien S, et al. High-dose imatinib mesylate therapy in newly diagnosed Philadelphia chromosome-positive chronic phase chronic myeloid leukemia. *Blood*. 2004;103: 2873-2878.
15. Kaneta Y, Kagami Y, Katagiri T, et al. Prediction of sensitivity to STI571 among chronic myeloid leukemia patients by genome-wide cDNA microarray analysis. *Jpn J Cancer Res*. 2002;93:849-856.
16. Quintas-Cardama A, Kantarjian H, O'Brien S, et al. Administration of G-CSF (filgrastim, Neupogen) for imatinib mesylate (Gleevec)-induced neutropenia in chronic phase chronic myeloid leukemia (CML) patients (pts) is safe and facilitates the achievement of cytogenetic responses [abstract]. *Blood*. 2003;102:907a. Abstract 3374.
17. O'Brien SG, Guilhot F, Larson RA, et al. Imatinib compared with interferon and low-dose cytarabine for newly diagnosed chronic-phase chronic myeloid leukemia. *N Engl J Med*. 2003;348:994-1004.
18. Kantarjian HM, Schiffer CA, Sawyer CL, et al. Imatinib (Gleevec) maintains favorable long-term outcome in chronic-phase chronic myeloid leukemia (CML) for patients failing interferon-alpha (IFN): follow up of a phase II study [abstract]. *Blood*. 2003;102: 905a. Abstract 3368.
19. Marin D, Marktel S, Szydlo R, et al. Survival of patients with chronic-phase chronic myeloid leukemia on imatinib after failure on interferon alfa. *Lancet*. 2003;362:617-619.

American Journal of Hematology 77:223–228 (2004)

Immature Granulocyte Fraction in the Peripheral Blood Is a Practical Indicator for Mobilization of CD34$^+$ Cells

Mari Endo-Matsubara, Seishi Ogawa, Ko Sasaki, Tsuyoshi Takahashi, Shigeru Chiba,* and Hisamaru Hirai

Departments of Cell Therapy/Transplantation Medicine and Hematology/Oncology, University of Tokyo Hospital and Graduate School of Medicine, Tokyo, Japan

We propose a simple parameter that improves prediction of the number of CD34$^+$ cells in blood cells collected by apheresis for autologous peripheral blood stem cell (PBSC) transplantation following administration of granulocyte colony-stimulating factor. The percentage of immature granulocytes including myeloblasts, promyelocytes, myelocytes, and metamyelocytes (LSI for left-shift index) immediately prior to the start of each apheresis correlated with the number of CD34$^+$ cells in PBSC collections ($r = 0.79$, $P < 0.0001$, $Y = 0.227X - 0.99$, $R^2 = 0.623$) much better than did the white blood cell count ($r = 0.07$), currently the most commonly used predictor in deciding the initiation of apheresis. We then used receiver operating characteristic (ROC) curves to determine a cutoff point for LSI to prevent unnecessary apheresis. At LSI > 7.5, sensitivity and specificity of cutoff points in the probability of obtaining >1.0 × 10^6 CD34$^+$ cells/kg BW were 93.3% and 94.3% (95% CI, 91.4–100.0%), respectively. When LSI reaches 15.25, nearly 100% of apheresis will attain the target CD34$^+$ cell dose. These findings indicate that LSI is a useful and simple method for predicting the yield of CD34$^+$ cells before the start of PBSC collection and avoiding unnecessary apheresis. Am. J. Hematol. 77:223–228, 2004. © 2004 Wiley-Liss, Inc.

Key words: peripheral blood stem cell transplantation; harvest; CD34$^+$ cells

INTRODUCTION

Autologous peripheral blood stem cell (PBSC) transplantation following high-dose chemotherapy is considered an effective curative strategy for a wide variety of malignancies resistant to conventional treatment or with poor prognostic factors [1–3]. Compared with bone marrow cells, PBSCs offer ease of collection and rapid rates of engraftment [4]. However, the timing of mobilization and yield are highly variable and thus the prediction of the number of mobilized stem cells in the peripheral blood (PB) is difficult. Such information is essential for deciding the optimal time for initiation of apheresis. A strong positive correlation is seen between the numbers of circulating CD34$^+$ cells and colony-forming unit granulocyte-macrophage (CFU-GM) [2,5,6], and it is now believed that the number of circulating CD34$^+$ cells is likely to represent the efficacy of stem cell mobilization. Therefore, the flow cytometry-based counting of CD34$^+$ cells in the peripheral blood is the most reliable method for initiating apheresis [7–9]. However, because of cost and lack of facilities in most clinical settings, monitoring CD34$^+$ cell number in PB has had little actual effect in avoiding unnecessary aphereses [10,11].

Many transplant centers start apheresis on a fixed day after the initiation of G-CSF administration (e.g., day 4 of G-CSF initiation) because of the low

Contract grant sponsor: Special Coordination Funds for Promoting Science and Technology from the Ministry of Education, Culture, Sports, Science and Technology of Japan, and Health; Contract grant sponsor: Labor Sciences Research Grants (Research Grants on Pharmaceutical and Medical Safety) from the Ministry of Health, Labor and Welfare of Japan; Contract grant numbers: KAKENHI 13307029, KAKENHI 14370300.

*Correspondence to: Shigeru Chiba, M.D., Department of Cell Therapy/Transplantation Medicine, University of Tokyo Hospital, Hongo, Tokyo 113-8655, Japan. E-mail: schiba-tky@umin.ac.jp

Received for publication 10 November 2003; Accepted 5 May 2004

Published online in Wiley InterScience (www.interscience.wiley.com). DOI: 10.1002/ajh.20193

probability of failure in stem cell harvest in this setting [12,13]. In other settings, however, the total white blood cell (WBC) count is frequently used as an indicator for the start of apheresis. The best time to begin PBSC collection after the chemotherapy-induced nadir without cytokine support is reported as the day of returning the WBC count to > 1,000/μL [14,15], while the WBC count > 3,000 or > 10,000/μL is recommended when cytokine support is combined [3,16]. The correlation between the WBC count and the number of $CD34^+$ cells in apheresis products, however, is not high, or even non-existent [8,17–20]. Therefore, there exists a need for a good indicator that can be obtained from ordinary clinical data that will reduce the frequencies of failed apheresis. Here, we report a retrospective analysis of the relationship between circulating $CD34^+$ cell number and the level of left shift of granulocytes in the blood.

PATIENTS AND METHODS

Patients

Forty-three consecutive patients with neoplastic diseases who underwent PBSC harvest after chemotherapy followed by G-CSF administration at our institution, between May 1995 and April 2000, were enrolled in the study. Patients with AML were excluded. All patients gave informed consent for the use of a small portion of blood.

Mobilization of PBSC

G-CSF (filgrastim) was given from 2 days after the completion of chemotherapy by single daily subcutaneous administration at 5 μg/kg until a day before the last PBSC apheresis. Apheresis was started using the AS104 continuous-flow blood cell separator (Fresenius AG, St. Wendel, Germany) when the WBC count reached 5,000/μL. At each apheresis, 150–200 mL of blood per kg was subjected to separation. The target cell dose for transplantation was 1×10^6 $CD34^+$ cells/kg actual body weight over 3 consecutive-day aphereses. Patients who failed to achieve the target cell dose underwent remobilization using alternative chemotherapy.

Evaluation for PBSC Graft

The two-color immunofluorescence-staining procedure and flow cytometric analysis have been performed as previously described. The number of $CD34^+$ cells was assessed by the SSC-FL method, i.e., the two-dimensional side scatter-fluorescence representation. The horizontal axis represents fluorescence of $CD34^+$ cells stained with HPCA2-PE antibody (Becton-Dickinson, Mountain View, CA), and the vertical axis represents side scatter. Flow-cytometric analysis was performed on a FACS Caliber (BDIS, San Jose, CA) in fresh samples obtained from each apheresis product. The instrument was operated with CaliBRITE beads (BDIS) and FACSomp software in lyse–wash mode (BDIS). For analysis of hematopoietic progenitor surface antigens in the PBSC harvest, a minimum of 100,000 events for each sample was collected using CellQuest software. In the cases of a large amount of CD34 weak-positive cells included, the cells to be measured were gated in the forward scatter (FCS)-CD45 Didot plot. To accomplish this, larger gates were first set on the CD34 weak-positive region using the CD34-side scatter dot plot. The gates include $CD34^+$ cells, lymphocytes, monocytes, and debris. Next, dual-color analyses of CD34 and CD45 antigens were performed for the gates to distinguish CD45 weak-positive progenitor cells from lymphocytes, monocytes, and debris.

Statistical Analysis

Most statistical analyses were performed with the Stat View statistical package (SAS, Cary, NC). The receiver operating characteristic (ROC) curve [23] was calculated with the SPSS statistical package (SPSS, Chicago, IL).

RESULTS

Patient Characteristics

Characteristics of the 43 patients (29 males, 14 females) included in the study are summarized in Table I. The median age was 39 years (range, 17–63 years). Twenty-nine patients had hematological malignancies, mostly non-Hodgkin's lymphoma.

PBSC Harvest Data

Thirty-one of 43 patients reached the target $CD34^+$ cell dose of 1×10^6/kg in the first series of mobilizations. In the 12 in whom $CD34^+$ cell dose was $< 1 \times 10^6$/kg, remobilization was performed in five, 4 of whom reached the goal with the second series. The median $CD34^+$ yield was 0.83×10^6/kg (range, $[0.041–22.5] \times 10^6$). The median number of apheresis procedures was 2 (range, 1–4) (Table I).

Predictors of Mobilization and Cell Yield

We next evaluated the relationship between the predictor candidates and $CD34^+$ cell numbers in the respective apheresis products. No correlation was found between $CD34^+$ cell numbers in respective harvests and total WBC count on the day of apheresis ($r = 0.07$, $n = 104$). The percentage of monocytes in WBC was previously reported to have a correlation

TABLE I. Patient Characteristics*

No. of patients	43
No. of apheresces	104
Median (range) age in years	39 (17–63)
Sex (male/female)	29/14
Diagnosis	
NHL	31
HD	3
ALL	4
MM	1
Germinoma	3
Uterine cancer	1
Pre-PBSC chemotherapy	
Cy	14
ETP	1
Ara-C	1
Cy/ETP	22
Ara-C/MIT	1
CHOP	2
Cy/ADM/CDDP	1
ETP/CDDP/Ara-C	2
CBDCA/Ara-C/ETP/MIT	3
MTX/IFM/CBDCA/ETP	1
Median (range) no. of apheresces	2 (1–4)
Median (range) WBC count just before harvest	11,700 (3,800–47,400)/μL
Median (range) no. of collected $CD34^+$ cells	0.83 (0.041–22.5) × 10^6/kg
No. who reached goal/no. who received chemotherapy	
1 course	31/43
2 courses	4/5

*Abbreviations: Cy, cyclophosphamide; ETP, etoposide; Ara-C, cytosine arabinoside; MIT, mitoxantron; ADM, adriamycin; CDDP, *cis*-diamine dichloroplatinum; IFM, ifosphamide; CBDCA, carboplatin.

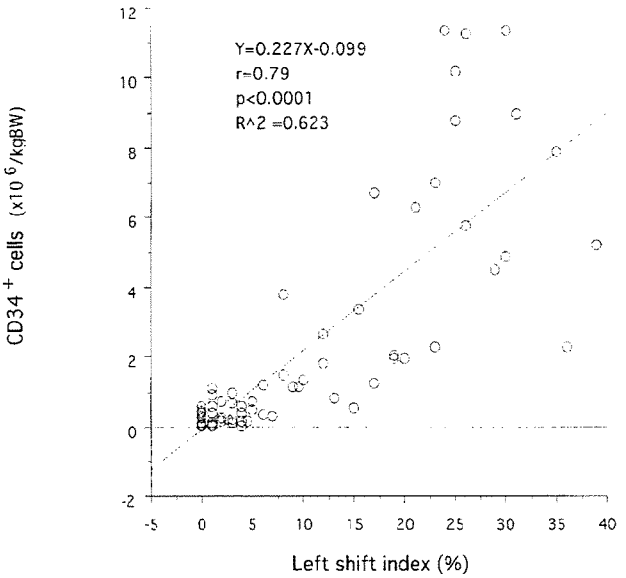

Fig. 1. Correlation analysis between Left Shift Index (LSI) and $CD34^+$ cells per apheresis product.

with the number of $CD34^+$ cells [9,24], but in our analysis there was no correlation ($r = 0.10$). In addition, no correlation was seen between the number of $CD34^+$ cells in respective harvests and the absolute reticulocyte counts ($r = 0.04$) on the day of apheresis. We also accessed the increase in WBC count on the day of apheresis as compared with the previous day and found a moderate correlation with the number of $CD34^+$ cells in respective harvests ($r = 0.46$, $P < 0.0001$, $R^2 = 0.215$).

We then assessed the correlation between the number of $CD34^+$ cells in respective harvests and differential percentages (%) on the day of apheresis. With the exception of the percentage of segmented neutrophils ($r = -0.68$), percentages of all differential components, i.e., myeloblasts, promyelocytes, myelocytes, metamyelocytes, and stabs, had a positive correlation with $CD34^+$ cell number ($r = 0.63$, 0.48, 0.76, 0.70, and 0.49, respectively). The sum of the percentages of myeloblasts, promyelocytes, myelocytes, and metamyelocytes, excluding stabs, showed a markedly high correlation ($r = 0.79$), being slightly better than that including stabs ($r = 0.77$). We therefore defined the former as left shift index (LSI) (Fig. 1; $r = 0.79$, $P < 0.0001$, $Y = 0.227X - 0.099$, $R^2 = 0.623$).

To render the LSI clinically usable, we evaluated ROC curves with the aim of establishing cutoff points for the optimal time to begin apheresis. The collection goal for transplantation is generally (1–2) × 10^6 $CD34^+$ cells/kg. Thus, practical goals for the number of $CD34^+$ cells from respective harvests could be 0.1 × 10^6 cells/kg, 0.25 × 10^6 cells/kg, 0.5 × 10^6 cells/kg, 1 × 10^6 cells/kg, etc. For each of the above goals, we examined ROC curves. The best cutoff point is at or near the "shoulder" of the ROC curve unless there are clinical reasons for minimizing either false negatives or false positives. According to this criterion, the best cutoff points of LSI for 0.1 × 10^6 cells/kg, 0.25 × 10^6 cells/kg, 0.5 × 10^6 cells/kg, and 1 × 10^6 cells/kg were 1.5%, 4.75%, 7.5%, and 7.5%, respectively (Fig. 2 and Table II). The cutoff point of 7.5% gives the sensitivity and specificity to obtain more than 1 × 10^6 cells/kg of 93.3% and 94.3%, respectively, meaning that only 6.7% of effective harvests are missed and only 5.6% of poor harvests will be falsely practiced. When LSI reaches more than 15.25%, nearly 100% of apheresis will attain the goal of 1 × 10^6 $CD34^+$ cells/kg. In our subjects, LSIs of 4.75%, 7.5%, and 15.25% were achieved in 35, 30, and 21 apheresis in a total of 66 apheresis trials, as summarized in Table III.

DISCUSSION

About 20–30% of patients fail to yield a sufficient number of $CD34^+$ cells to ensure prompt engraftment of neutrophils and platelets [25–29]. Apheresis failures

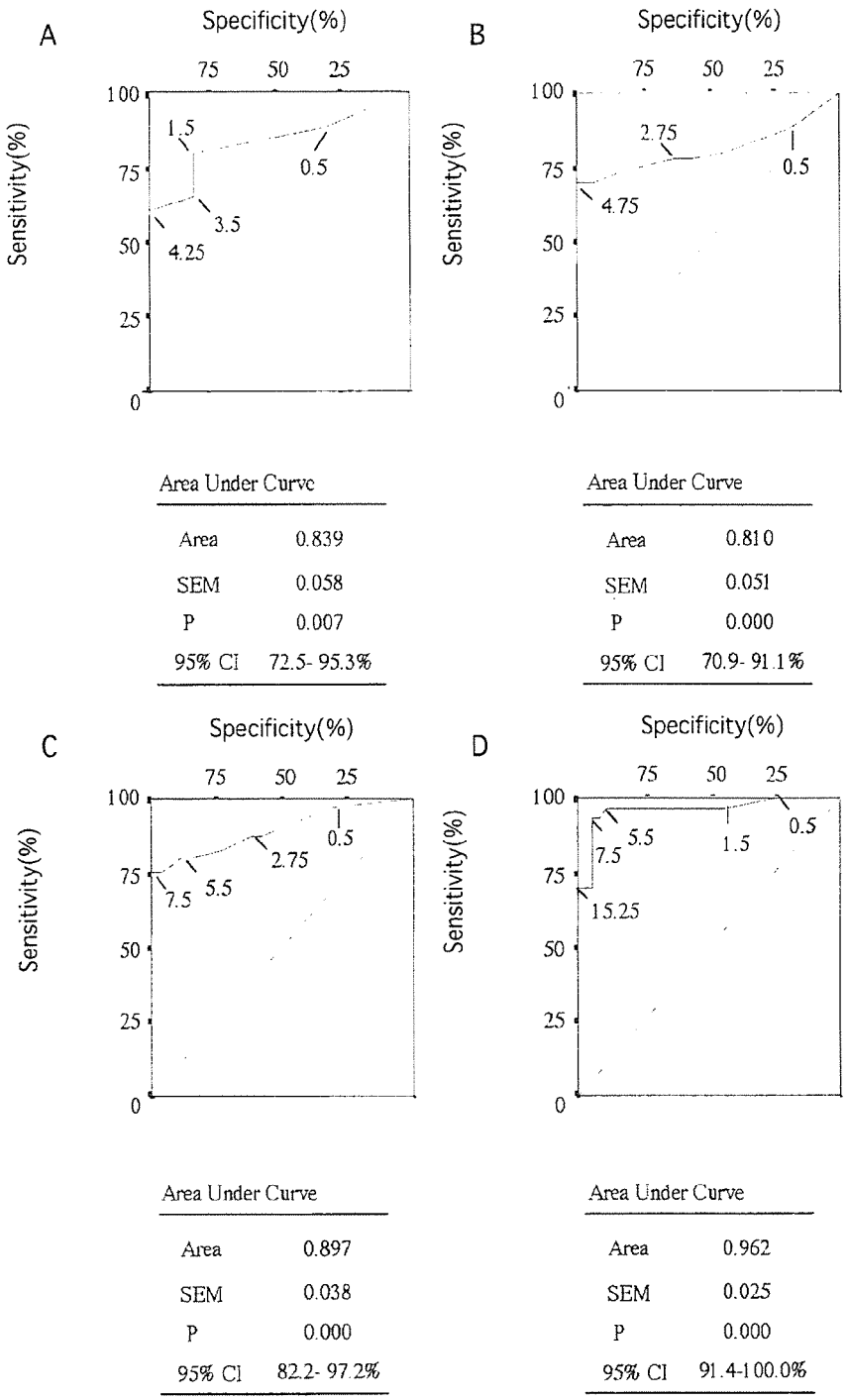

Area Under Curve	
Area	0.839
SEM	0.058
P	0.007
95% CI	72.5- 95.3%

Area Under Curve	
Area	0.810
SEM	0.051
P	0.000
95% CI	70.9- 91.1%

Area Under Curve	
Area	0.897
SEM	0.038
P	0.000
95% CI	82.2- 97.2%

Area Under Curve	
Area	0.962
SEM	0.025
P	0.000
95% CI	91.4-100.0%

Fig. 2. Receiver operating characteristic (ROC) curve of LSI for the prediction of sufficient or poor harvest. Target cell doses per apheresis are 0.1 × 10^6/kg BW (A), 0.25 × 10^6/kg BW (B), 0.5 × 10^6/kg BW (C), and 1.0 × 10^6/kg BW (D). Abbreviations: AUC; area under curve, SEM; standard error of the mean, P; probability, CI; confidence interval.

can be reduced if reliable indicators are available for measuring adequate mobilization of $CD34^+$ cells.

The WBC count during the recovery phase following the chemotherapy-induced nadir is widely used as the practical indicator of time to initiate apheresis, but the counts do not correlate well with the number of mobilized $CD34^+$ cells [18–20,30,31]. Several previous studies reported that the rate of WBC recovery

TABLE II. Sensitivity, Specificity, Positive, and Negative Predictive Values at the Cutoff Point of LSI in Four Kinds of Target Cell Dosage for Respective Harvest

	Target cell dosage for respective harvest (/kg BW)			
	0.1×10^6	0.25×10^6	0.5×10^6	1.0×10^6
Cutoff point of LSI (%)	1.5	4.75	7.5	7.5
Sensitivity (%)	80.0	70.0	75.0	93.3
Specificity (%)	83.3	100	100	94.3
Predictive value of positive test (%)	98.0	100	100	93.3
Predictive value of negative test (%)	29.4	51.6	72.2	94.3

TABLE III. Frequency of Achievements for the Cutoff Points of LSI

Apheresis no.	LSI > 4.75/ total (%)	LSI > 7.5/ total (%)	LSI > 15.25/ total (%)
1st apheresis	22/33 (66.7%)	19/33 (57.6%)	13/33 (39.4%)
2nd apheresis	11/22 (50.0%)	9/22 (40.9%)	8/22 (36.4%)
3rd apheresis	2/8 (25%)	2/8 (25%)	NA
4th apheresis	0/3 (0%)	NA	NA

NA, not applicable.

could be used to predict the most effective time for apheresis [5,9,27,32,33], but in our experience, the correlation between WBC recovery rate and the $CD34^+$ cell number was moderate, indicating that this parameter is not useful in clinical practice.

Some investigators reported that pre-apheresis $CD34^+$ cell counts reliably predict $CD34^+$ cell yields. Haas et al. showed a strong correlation ($r = 0.80$) between them in 142 collections performed for 61 lymphoma patients after chemotherapy and cytokine mobilization [34]. Nevertheless, a great majority of institutions still use WBC counts or the rate of increase in the WBC count during G-SCF-assisted recovery after chemotherapy to predict the timing for optimal PBSC collection, because not all institutions have the capability to rapidly measure $CD34^+$ counts [10,11]. We could say collections have depended to empirical knowledge of clinicians in the latter institutions.

The simple sum of the percentages of immature granulocytes, proposed as LSI here, is superior to others not only in terms of its remarkably high (similar to pre-apheresis $CD34^+$ cell counts!) correlation with $CD34^+$ cell number ($r = 0.79$, $P < 0.0001$) but in terms of the adaptability to heavily pretreated patients as well. Moreover, our regression analysis has also established concrete cutoff points, which helps decisions to cease or continue collection, leads to good cost performance.

This report is a retrospective study, so we suggest that prospective studies be performed in many institutions.

ACKNOWLEDGMENTS

This work was supported in part by grants-in-aid and Special Coordination Funds for Promoting Science and Technology from the Ministry of Education, Culture, Sports, Science and Technology of Japan, and Health and Labor Sciences Research Grants (Research Grants on Pharmaceutical and Medical Safety) from the Ministry of Health, Labor and Welfare of Japan.

REFERENCES

1. Barlogie B, Shaughnessy J, Tricot G, et al. Treatment of multiple myeloma. Blood 2004;103:20–32.
2. Bender JG, Williams SF, Myers S, et al. Characterization of chemotherapy mobilized peripheral blood progenitor cells for use in autologous stem cell transplantation. Bone Marrow Transplant 1992;10:281–285.
3. Kotasek D, Shepherd KM, Sage RE, et al. Factors affecting blood stem cell collections following high-dose cyclophosphamide mobilization in lymphoma, myeloma and solid tumors. Bone Marrow Transplant 1992;9:11–17.
4. Attal M, Harousseau JL, Stoppa AM, et al. A prospective, randomized trial of autologous bone marrow transplantation and chemotherapy in multiple myeloma. Intergroupe Français du Myelome. N Engl J Med 1996;335:91–97.
5. Craig JI, Anthony RS, Stewart A, Thomson EB, Gillon J, Parker AC. Peripheral blood stem cell mobilization using high-dose cyclophosphamide and G-CSF in pretreated patients with lymphoma. Br J Haematol 1993;85:210–212.
6. Siena S, Bregni M, Brando B, et al. Flow cytometry for clinical estimation of circulating hematopoietic progenitors for autologous transplantation in cancer patients. Blood 1991;77:400–409.
7. Bensinger W, Singer J, Appelbaum F, et al. Autologous transplantation with peripheral blood mononuclear cells collected after administration of recombinant granulocyte stimulating factor. Blood 1993;81:3158–3163.
8. Hénon PH, Sovalat H, Bourderont D. Importance of $CD34^+$ cell subsets in autologous PBSC transplantation: the Mulhouse experience using $CD34^+CD38^-$ cells as predictive tool for hematopoietic engraftment. J Biol Regul Homeost Agents 2001;15:62–67.
9. Moncada V, Bolan C, Yau YY, Leitman SF. Analysis of PBPC cell yields during large-volume leukapheresis of subjects with a poor mobilization response to filgrastim. Transfusion 2003;43: 495–501.
10. Elias AD, Ayash L, Anderson KC, et al. Mobilization of peripheral blood progenitor cells by chemotherapy and granulocyte-macrophage colony-stimulating factor for hematologic support after high-dose intensification for breast cancer. Blood 1992;79: 3036–3044.
11. Zimmerman TM, Lee WJ, Bender JG, Mick R, Williams SF. Quantitative CD34 analysis may be used to guide peripheral blood stem cell harvests. Bone Marrow Transplant 1995;15: 439–444.
12. Alegre A, Tomas JF, Martinez-Chamorro C, et al. Comparison of peripheral blood progenitor cell mobilization in patients with multiple myeloma: high-dose cyclophosphamide plus GM-CSF vs. G-CSF alone. Bone Marrow Transplant 1997;20:211–217.
13. Desikan KR, Barlogie B, Jagannath S, et al. Comparable engraftment kinetics following peripheral-blood stem-cell infusion mobilized with granulocyte colony-stimulating factor with or without cyclophosphamide in multiple myeloma. J Clin Oncol 1998;16: 1547–1553.

14. Gianni AM, Siena S, Bregni M, et al. Granulocyte-macrophage colony-stimulating factor to harvest circulating haemopoietic stem cells for autotransplantation. Lancet 1989;2:580–585.
15. To LB, Shepperd KM, Haylock DN, et al. Single high doses of cyclophosphamide enable the collection of high numbers of haemopoietic stem cells from the peripheral blood. Exp Hematol 1990; 18:442–447.
16. Bensinger W, Appelbaum F, Rowley S, et al. Factors that influence collection and engraftment of autologous peripheral-blood stem cells. J Clin Oncol 1995;13:2547–2555.
17. Gordan LN, Sugrue MW, Lynch JW, et al. Poor mobilization of peripheral blood stem cells is a risk factor for worse outcome in lymphoma patients undergoing autologous stem cell transplantation. Leuk Lymphoma 2003;44:815–820.
18. Kiss JE, Rybka WB, Winkelstein A, et al. Relationship of $CD34^+$ cell dose to early and late hematopoiesis following autologous peripheral blood stem cell transplantation. Bone Marrow Transplant 1997;19:303–310.
19. Remacha AF, Martino R, Sureda A, et al. Changes in reticulocyte fractions during peripheral stem cell harvesting: role in monitoring stem cell collection. Bone Marrow Transplant 1996;17:163–168.
20. Teshima T, Harada M, Takamatsu Y, et al. Cytotoxic drug and cytotoxic drug/G-CSF mobilization of peripheral blood stem cells and their use for autografting. Bone Marrow Transplant 1992;10: 215–220.
21. Morii T, Nishikawa K, Shimoyama T, et al. Quantitative flow-cytometric analysis of CD34-positive stem cells in peripheral blood stem cell harvests. Rinsho Ketsueki 1994;35:649–656 [in Japanese].
22. Miyazaki T, Matsuda I, Oguri M, et al. Flow cytometric analysis of hematopoietic progenitor cells in peripheral blood stem cell harvest from patients with CD34-positive acute leukemia. J Immunol Methods 2001;247:9–15.
23. Metz CE. Basic principles of ROC analysis. Semin Nucl Med 1978;8:283–298.
24. Okada Y, Ando M, Kato T, et al. Characteristics of blood cells during peripheral blood stem cell mobilization following chemotherapy in patients with non-Hodgkin's lymphoma. Rinsho Ketsueki 2000;41:91–96 [in Japanese].
25. Armitage S, Hargreaves R, Samson D, Brennan M, Kanfer E, Navarrete C. CD34 counts to predict the adequate collection of peripheral blood progenitor cells. Bone Marrow Transplant 1997; 20:587–591.
26. Gazitt Y, Freytes CO, Callander N, et al. Successful PBSC mobilization with high-dose G-CSF for patients failing a first round of mobilization. J Hematother 1999;8:173–183.
27. Ketterer N, Salles G, Moullet I, et al. Factors associated with successful mobilization of peripheral blood progenitor cells in 200 patients with lymphoid malignancies. Br J Haematol 1998; 103:235–242.
28. Lie AK, Hui CH, Rawling T, et al. Granulocyte colony-stimulating factor (G-CSF) dose-dependent efficacy in peripheral blood stem cell mobilization in patients who had failed initial mobilization with chemotherapy and G-CSF. Bone Marrow Transplant 1998;22:853–857.
29. Weaver CH, Tauer K, Zhen B, et al. Second attempts at mobilization of peripheral blood stem cells in patients with initial low $CD34^+$ cell yields. J Hematother 1998;7:241–249.
30. To LB, Roberts MM, Haylock DN, et al. Comparison of haematological recovery times and supportive care requirements of autologous recovery phase peripheral blood stem cell transplants, autologous bone marrow transplants and allogeneic bone marrow transplants. Bone Marrow Transplant 1992;9:277–284.
31. Yu J, Leisenring W, Bensinger WI, Holmberg LA, Rowley SD. The predictive value of white cell or $CD34^+$ cell count in the peripheral blood for timing apheresis and maximizing yield. Transfusion 1999;39:442–450.
32. Kasparu H, Krieger O, Girschikofsky M, Kolb A, Bettelheim P, Lutz D. Factors influencing the timing of peripheral blood stem cell collection (PBSC). Transfus Sci 1996;17:595–600.
33. Williams O, Demirer T, Lilleby K, Buckner CD, Bensinger WI. Tempo of hematologic recovery correlates with peripheral blood $CD34^+$ cell level in patients undergoing stem cell mobilization. J Clin Apheresis 1998;13:1–6.
34. Haas R, Mohle R, Fruhauf S, et al. Patient characteristics associated with successful mobilizing and autografting of peripheral blood progenitor cells in malignant lymphoma. Blood 1994;83:3787–3794.

THE JOURNAL OF BIOLOGICAL CHEMISTRY
Vol. 279, No. 15, Issue of April 9, pp. 15630–15638, 2004
Printed in U.S.A.

AML1 Is Functionally Regulated through p300-mediated Acetylation on Specific Lysine Residues*

Received for publication, January 13, 2004
Published, JBC Papers in Press, January 29, 2004, DOI 10.1074/jbc.M400355200

Yuko Yamaguchi‡, Mineo Kurokawa‡‖, Yoichi Imai‡, Koji Izutsu‡, Takashi Asai‡, Motoshi Ichikawa‡, Go Yamamoto‡, Eriko Nitta‡, Tetsuya Yamagata‡, Kazuki Sasaki§, Kinuko Mitani¶, Seishi Ogawa‡, Shigeru Chiba‡, and Hisamaru Hirai†‡

From the ‡Department of Hematology and Oncology, Graduate School of Medicine, University of Tokyo, Tokyo 113-8655, the §Growth Factor Division, National Cancer Center Research Institute, Tokyo 104-0045, and the ¶Department of Hematology, Dokkyo University School of Medicine, Mibu, Tochigi 321-0293, Japan

***AML1* (*RUNX1*) is one of the most frequently disrupted genes in human leukemias. *AML1* encodes transcription factors, which play a pivotal role in hematopoietic differentiation, and their inappropriate expression is associated with leukemic transformation of hematopoietic cells. Previous studies demonstrated that the transcription cofactor p300 binds to the C-terminal region of AML1 and stimulates AML1-dependent transcription during myeloid cell differentiation. Here, we report that AML1 is specifically acetylated by p300 *in vitro*. Mutagenesis analyses reveal that p300 acetylates AML1 at the two conserved lysine residues (Lys-24 and Lys-43). AML1 is subject to acetylation at the same sites *in vivo*, and p300-mediated acetylation significantly augments the DNA binding activity of AML1. Disruption of these two lysines severely impairs DNA binding of AML1 and reduced the transcriptional activity and the transforming potential of AML1. Taken together, these data indicate that acetylation of AML1 through p300 is a critical manner of posttranslational modification and identify a novel mechanism for regulating the function of AML1.**

AML1 (PEBP2αB, core binding factor α2, or RUNX1) and its cofactor PEBP2β/core binding factor β are the most frequent targets of chromosomal translocations in human leukemias (1). The *AML1* gene was identified through its involvement in the (8;21) translocation, which rearranges the *AML1* gene on chromosome 21q22 and the *ETO* (*MTG8*) gene on chromosome 8q22, resulting in the generation of the AML1-ETO fusion protein (2–4). *AML1* is also involved in human leukemias carrying t(3;21) or t(12;21) translocation, suggesting that it plays an important role in leukemogenesis (5–8).

The *AML1* gene encodes a transcription factor containing an N-terminal DNA-binding domain that is highly homologous to the *Drosophila* pair-rule protein Runt, which is called the Runt domain (9). AML1 binds to the core enhancer DNA sequence, TG(T/c)GGT, called the PEBP2 site, through the Runt domain. Its affinity for DNA is markedly increased by heterodimerization with PEBP2β (10–13). This heterodimeric complex regulates transcription of a large number of hematopoietic lineage-specific genes (14, 15). Targeted disruption of either *AML1* or *PEBP2β* has demonstrated that both AML1 and PEBP2β are essential for all lineages of definitive hematopoiesis in the murine fetal liver (16–18). In addition, AML1 exhibits the transforming activity when expressed in fibroblasts, and this activity requires both the Runt domain and the C-terminal transcriptional regulatory domain called the PST region (19). At least four forms of the AML1 proteins are produced by alternative splicing, termed AML1a, AML1b, AML1c, and AML1ΔN (20, 21). Among them, AML1b is one of the transcriptionally active forms, which contain both the Runt domain and the PST region (22). We simply refer to this alternative form as AML1 hereafter.

Previously, Kitabayashi *et al.* (23) demonstrated that AML1 associates with a transcription cofactor p300 *in vivo* and that p300 potentiates AML1-dependent transcriptional activation. On the other hand, AML1 synergizes with a variety of transcription factors, including CCAAT/enhancer binding protein-α, AP-1, Ets-1, PU.1, and c-Myb, which regulate cellular proliferation and differentiation (24–30). Conversely, AML1 can repress transcription by associating with corepressors such as Groucho/transducin-like Enhancer of split and mSin3A (31–33). Thus, AML1 appears to act as an "organizing" factor of transcription by interacting with a wide variety of transcription regulators. In contrast, regulatory mechanisms for AML1 function remain elusive thus far. Previously, we reported that AML1 is phosphorylated through the extracellular signal-regulated kinase (ERK)[1] (34). ERK-dependent phosphorylation potentiates the transactivation ability and the transforming capacity of AML1 through regulating interaction between AML1 and mSin3A (35). Thus, the function of AML1 is also regulated through the signal transduction pathways.

Acetylation has recently emerged as the central mode of regulation for a significant number of transcription factors (36, 37). p300 and the related protein CBP are highly conserved proteins that have a pivotal role in transcriptional regulation, bridging a wide variety of DNA-binding proteins to components of the general transcriptional machinery (38). In addition, p300

* This work was partially supported by a fellowship from the Ministry of Education, Culture, Sports, Science and Technology of Japan. The costs of publication of this article were defrayed in part by the payment of page charges. This article must therefore be hereby marked "*advertisement*" in accordance with 18 U.S.C. Section 1734 solely to indicate this fact.

†Hisamaru Hirai died suddenly on August 23, 2003. His students, fellows, and colleagues will greatly miss his energetic and nurturing leadership in the field of hematology. We dedicate this paper in his memory.

‖ To whom correspondence should be addressed: Dept. of Hematology and Oncology, Graduate School of Medicine, University of Tokyo, 7-3-1 Hongo, Bunkyo-ku, Tokyo 113-8655, Japan. Tel.: 81-3-5800-6528; Fax: 81-3-3815-8350; E-mail: kurokawa-tky@umin.ac.jp.

[1] The abbreviations used are: ERK, extracellular signal-regulated kinase; HAT, histone acetyltransferase; GST, glutathione *S*-transferase; EMSA, electrophoretic mobility shift assay; CBP, CREB-binding protein; CREB, cAMP-response element-binding protein; luc, luciferase; PST region, a proline-, serine-, and threonine-rich region; P/CAF, p300/CBP-associated factor; M-CSF receptor, macrophage colony-stimulating factor receptor.

and CBP possess histone acetyltransferase (HAT) activity, which is able to acetylate histone and non-histone proteins. Histone acetylation is linked to transcriptional activation and participates in the nucleosomal remodeling that accompanies gene activity (39). Recently, HATs have been shown to also acetylate a significant number of non-histone proteins, which include transcription factors such as p53, *Drosophila* T-cell receptor, erythroid kruppel-like factor, GATA-1, GATA-3, and the high mobility group protein I/Y (40, 41). Acetylation of these factors leads to changes in protein-protein and protein-DNA interaction, which subsequently result in altered gene expression (42). Here we report that AML1 is acetylated by p300 at the two lysine residues located in the N terminus adjacent to the Runt domain. Acetylation of AML1 significantly increases the amount of AML1 bound to DNA and results in stimulation of AML1-dependent transcription. Substitution of target residues uncovered a close relationship between the acetylation and the *in vivo* function of AML1. Our studies demonstrate that acetylation is a critical manner of posttranslational modification of AML1.

MATERIALS AND METHODS

Cell Cultures—COS7, 293T, HeLa, and NIH3T3 cells were maintained in Dulbecco's modified Eagle's medium supplemented with penicillin, streptomycin, and 10% fetal calf serum at 37 °C in a 5% CO_2 incubator. M1 cells and MOLT-4 cells were cultured in Dulbecco's modified Eagle's medium and α-minimal essential medium by one to one and RPMI 1640 medium, respectively, which contain penicillin, streptomycin, and 10% fetal calf serum.

Plasmid Constructions and Recombinant Proteins—pGEX-AML1-(1–189), pGEX-K24R/K43R-(1–189), and pGEX-K24A/K43A-(1–189) were obtained by cloning the PCR fragments corresponding to amino acids 1–189 of AML1, K24R/K43R, and K24A/K43A into the pGEX2T vector, respectively. For construction of FLAG-tagged P/CAF-HAT/Br and GCN5, the DNA fragments corresponding to amino acids 352–832 and amino acids 1–477, respectively, were amplified by PCR and subcloned into pFLAG-MAC (Kodak). The expression plasmids for GST-PEBP2β and FLAG-tagged p300-HAT were constructed as described previously (43, 44). Construction of pME18S-AML1 and AML1Δ-(47–172) was described elsewhere (19, 45). For construction of Δ-(23–64), a fragment for amino acids 1–64 of AML1 was replaced by a fragment for amino acids 1–22 generated by a PCR method. For construction of Δ-(173–188), the ApaI-SalI fragment of AML1 was replaced by the corresponding fragment that lacks the region between amino acids 173 and 188, which was generated by a PCR method. For tagging AML1 and deletion mutants at the N terminus, the FLAG octapeptide (DYKDDDDK) was inserted after the first methionine by PCR as described previously (32). The AML1 K24R, K43R, K24R/K43R, K24A/K43A, K182R, K188R, and K182R/K188R were obtained by replacing the lysine residues with arginines and alanines, respectively, by the site-directed mutagenesis method (46). For construction of the retroviral vector that harbors AML1 or K24A/K43A, the 1.8-kb EcoRI fragment encoding AML1 or K24A/K43A was deprived of the polyadenylation signal by digestion with BamHI and cloned into the pSRαMSVtk*neo* vector (19). pM-CSF-R-luc containing −416 to +71 of the human M-CSF receptor promoter was described previously (47). pcDEF3-p300 was kindly provided by Dr. Miyazono and Dr. Kawabata. The glutathione *S*-transferase (GST) fusion constructs of AML1, FLAG-tagged p300-HAT, P/CAF-HAT/Br, and GCN5 were purified as described previously (44, 45).

In Vitro Acetylation Assays—GST fusion proteins or histones (Roche Applied Science) were collected on glutathione-Sephahrose beads (Amersham Biosciences), incubated at 30 °C for 1 h in the buffer containing 50 mM Tris, pH 8.0, 10% glycerol, 1 mM dithiothreitol, 1 mM phenylmethylsulfonyl fluoride, 10 mM sodium butyrate, and 0.05 μCi of [^{14}C]acetyl-CoA (Amersham Biosciences), and analyzed by sodium dodecyl sulfate-polyacrylamide gel electrophoresis (SDS-PAGE).

Transfection, Immunoprecipitation, and Immunoblot Analysis—COS7 cells or 293T cells were transfected with expression plasmids by the DEAE-dextran method as described previously (48). Polyclonal antisera to the full-length (anti-AML1), the PST region (anti-PST) of AML1, and PEBP2β (anti-PEBP2β) were raised in rabbit against bacterially produced proteins as described previously (43, 45, 49). For detection of p300 and AML1 proteins, the indicated cells were lysed in the buffer containing 350 mM NaCl, 50 mM Tris-HCl (pH 7.5), 0.5% Igepal, 1 mM EDTA, 0.5 mM dithiothreitol, 10 mM sodium butyrate, 1 μg of aprotinin/ml, 1 μg of pepstatin/ml, 1 μg of leupeptin/ml, 0.2 mM phenylmethylsulfonyl fluoride followed by incubation for 30 min on ice. Whole cell lysates containing 100 μg of proteins were subjected to SDS-PAGE and transferred to polyvinylidene difluoride membranes (Immobilon, Millipore). The membranes were blocked with 10% skim milk, treated with anti-p300 (RW128, Upstate Biotechnology), anti-AML1, anti-FLAG (M2; Sigma), or anti-PEBP2β, washed, and reacted with the mouse or rabbit anti-IgG antibody coupled to horseradish peroxidase. The blots were visualized using the enhanced chemiluminescence (ECL) system (Amersham Biosciences). For immunoprecipitation, cells were lysed in the above buffer and subjected to immunoprecipitation with anti-PST or anti-AML1 (PC284L; Oncogene) followed by absorption to protein A-Sepharose (Sigma). Immunoprecipitates were washed, separated by SDS-PAGE, and analyzed with anti-p300 as described above.

In Vivo Sodium [^{3}H]Acetate Labeling—MOLT-4 cells were grown to 2×10^7 cells, washed twice with cold phosphate-buffered saline, resuspended in RPMI labeling medium (1 mCi of ^{3}H-sodium acetate (Amersham Biosciences) per ml and 50 nM trichostatin A (Wako)), and then incubated at 37 °C for 90 min. pME18S-AML1 and mutants either with or without FLAG tag were transfected with pcDEF3-p300 as described above into COS7 cells. After 30 h, cells were exposed to 1 mCi of sodium [^{3}H]acetate/ml in the presence of 50 nM trichostatin A for 90 min. Lysates were prepared and processed using either anti-PST or anti-FLAG as described above and resolved by SDS-PAGE. Proteins were electrotransferred onto polyvinylidene difluoride membrane (Immobilon, Millipore) and analyzed using BAS2000 Image Analyzer (Fuji Film).

Electrophoretic Mobility Shift Assay (EMSA)—The M4 probe containing a partial A core of the polyomavirus enhancer was produced as described elsewhere (50). Five micrograms of GST fusion proteins were collected on glutathione-Sepharose beads, incubated with purified FLAG-p300-HAT in the presence or absence of 10 nM acetyl-CoA (Amersham Biosciences). Then, reaction mixtures were eluted from the beads in glutathione elution buffer (10 mM reduced glutathione in 50 mM Tris-HCl (pH 8.0)). GST-PEBP2β collected on glutathione-Sepharose beads was incubated in the thrombin (Amersham Biosciences) reaction mixture at room temperature for 16 h, and then centrifuged, and supernatant containing PEBP2β cleaved off from GST was collected. The recovered proteins were quantified by Coomassie staining, and 100 ng of these proteins were incubated with 1 ng of M4 probe in the buffer containing 20 mM Hepes (pH 7.6), 4% Ficoll (W/V), 10 mM EDTA, 40 mM KCl, 0.5 mM dithiothreitol, 300 ng of poly(dI-dC) for 30 min at room temperature in the presence or absence of PEBP2β. Seventy ng of unlabeled M4 probe were added as a cold competitor. Reaction mixtures were subjected to EMSA as described previously (45). Nuclear extracts were obtained from COS7 cells transfected with full-length AML1 or K24R/K43R in pME18S either alone or together with PEBP2β by the DEAE-dextran method, as described previously (19). The procedures for EMSA were presented previously (45). For radioisotope labeling, [α-^{32}P]dCTP was incorporated into the M4 probe by incubating with the Klenow fragment.

Luciferase Assays—HeLa cells were transfected by using SuperFect (Qiagen) with pM-CSF-R-luc and plasmids expressing wild type AML1, K24R/K43R, or K24A/K43A in the presence or absence of p300 expression plasmids. Fifty ng/ml trichostatin A was added 8 h prior to harvest. Luciferase activity was determined 48 h later, as described previously (51). A plasmid expressing β-galactosidase was co-transfected as an internal control of transfection efficiency, and the data were normalized to the β-galactosidase activity, as described previously (51).

Soft Agar Assays—Soft agar assays were performed according to procedures described elsewhere (19, 52). Colonies were counted after 14 days of culture in soft agar if they were larger than 0.25 mm in diameter.

RESULTS

AML1 Interacts with p300 in Vivo—p300 and CBP are known to interact with a variety of transcriptional factors as coactivators. Recently, a physical interaction between AML1 and p300 was demonstrated (23). To confirm the interaction of endogenous AML1 with p300 in hematopoietic cells, we performed immunoprecipitation experiments using M1 cells, a murine leukemic cell line. Whole cell lysates were prepared from M1 cells and subjected to immunoprecipitation with the anti-AML1 antibody or control preimmune serum. Immunoblot

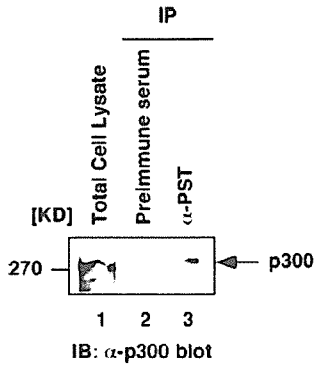

FIG. 1. **AML1 interacts with p300 *in vivo*.** Co-immunoprecipitation (*IP*) of endogenous AML1 with p300 in lysates from M1 cells is shown. Whole cell lysates were precipitated with preimmune serum (*lane 2*) or anti-PST serum (*lane 3*), and the precipitate was subjected to immunoblot (*IB*) analysis with anti-p300.

analysis with the p300-specific antibody showed that the precipitate with anti-AML1 contained p300, whereas p300 protein was never detected in the precipitate obtained with control preimmune serum (Fig. 1). These results indicate that AML1 forms complexes with p300 *in vivo* in agreement with previous findings (23).

p300 Specifically Acetylates AML1 in Vitro—Association of p300 with AML1, together with the recent demonstration of its acetyltransferase activity on a variety of transcription factors, prompted us to determine whether AML1 is a substrate for acetylation by p300. AML1 possesses nine lysine residues, which become potential targets for acetylation. To examine whether AML1 could be acetylated by p300 directly, the *in vitro* acetylation assays were performed using bacterially expressed FLAG-tagged HAT domain of p300 (p300-HAT). GST was fused to a region between amino acids 1 and 189 of AML1 (AML1-(1–189)), which contains all nine lysine residues, and the GST fusion protein was expressed in the BL21 bacterial host and purified (Fig. 2*A*). GST-AML1-(1–189) was incubated with p300-HAT in the presence of [^{14}C]acetyl-CoA. Use of these highly purified recombinant proteins eliminates possible contamination by other HATs. As shown in Fig. 2*B*, GST-AML1-(1–189) was specifically labeled with [^{14}C]acetyl-CoA in the presence of p300-HAT, whereas no signal was detected for GST alone. The faster migrating bands were considered to represent degraded products of the acetylated AML1 protein because the purified GST-AML1-(1–189) that served as a substrate contains identically migrating bands. In contrast, GST-AML1-(1–189) was never labeled without p300-HAT. We further investigated whether other HATs can acetylate AML1 using P/CAF and its close homologue GCN5. The HAT/bromodomain of P/CAF (P/CAF-HAT/Br) and full-length GCN5 were tagged with FLAG, expressed bacterially, and subsequently used in the *in vitro* acetylation assays. The results in Fig. 2*B* show that neither P/CAF-HAT/Br nor GCN5 acetylated GST-AML1-(1–189) at all. As shown in Fig. 2*C*, the HAT activities of p300-HAT, P/CAF-HAT/Br, and GCN5 were confirmed by using histones as substrates. p300-HAT could acetylate histones H2A, H2B, H3, and H4, whereas only histones H3 and H4 were acetylated by P/CAF-HAT/Br and GCN5, which is in agreement with the previous reports (42). Taken together, these results unequivocally indicate that AML1 can be a specific substrate for p300-mediated acetylation *in vitro*.

In Vivo Acetylation of AML1—Next, we went on further to examine whether acetylation of AML1 occurs *in vivo* to manifest a physiological relevance of *in vitro* acetylation of AML1. First, we wished to determine whether endogenous AML1 in hematopoietic cells was also acetylated. For these experiments, we pulse-labeled MOLT-4 cells, a human acute lymphoblastic leukemia cell line, with [^{3}H]acetate in the presence of a histone deacetylase inhibitor (trichostatin A) and then subjected them to cell lysis and immunoprecipitation with anti-AML1. As shown in Fig. 3*A*, anti-AML1, but not control preimmune serum, precipitated [^{3}H]acetate-labeled AML1 (*lanes 2* and *3*). Immunoblot analysis with the same antibody revealed migration of endogenous AML1 (*lane 1*). These results directly provide evidence that AML1 is endogenously acetylated in hematopoietic cells.

To define the positions within AML1 to be acetylated by p300, we then employed transient transfection into COS7 cells. First, cells were transfected with FLAG-tagged full-length AML1 and p300 and labeled with sodium [^{3}H]acetate in the same manner performed above. Lysates were immunoprecipitated with the anti-FLAG antibody and subjected to immunoblot analysis. As shown in Fig. 3*B*, AML1 was efficiently recovered from AML1-transfected cells with anti-FLAG. The immunoprecipitated AML1 protein was specifically labeled with [^{3}H]acetate as in MOLT-4 cells (Fig. 3*B*, *right*). Next, we employed three types of serial deletion mutants to cover all nine lysines (Fig. 2*A*). These FLAG-tagged mutants were expressed in COS7 cells together with p300 and subjected to the *in vivo* acetylation assays. Fig. 3*B* shows that these mutants are expressed in COS7 cells in the anticipated sizes. Acetylation of AML1 was retained when amino acids 47–172 in the Runt domain or amino acids 173–188 in C-terminal region adjacent to the Runt domain are deleted (*lanes 9* and *10*). In contrast, deletion of N-terminal region (amino acids 23–64) flanked by the Runt domain completely abolished AML1 acetylation by p300 (*lane 8*). This region contains two lysine residues, Lys-24 and Lys-43. These two lysines are highly conserved among the Runt-containing protein family, with Lys-24 being completely conserved from the Zebrafish Runx1 to the human AML1 family members. These results suggest that either or both of these two N-terminal lysines are potentially acetylated by p300.

AML1 Is Acetylated by p300 on N-terminal Two Lysine Residues—To precisely determine the target residues of AML1 for p300-mediated acetylation, Lys-24 and Lys-43 were substituted with arginines or alanines either individually or in combination. Substitution of either Lys-24 or Lys-43 with arginine (K24R or K43R) significantly reduced the level of acetylation. The level of acetylation in K24R was significantly lower than that in K43R. Furthermore, substitution of both Lys-24 and Lys-43 by arginines or alanines almost completely abolished acetylation of AML1 (Fig. 4*B*). In contrast, substitution of C-terminal lysines (Lys-182 and Lys-188) did not alter *in vivo* acetylation of AML1, indicating that these residues are not involved in acetylation. These findings suggest that Lys-24 and Lys-43 are preferentially acetylated *in vivo* in agreement with the results obtained from the deletion mutants. We also performed an *in vitro* acetylation assay using purified forms of GST-K24R/K43R-(1–189) and GST-K24A/K43A-(1–189) in which Lys-24 and Lys-43 of AML1-(1–189) were substituted by arginines and alanines, respectively. Although GST-AML1-(1–189) was efficiently acetylated by p300, no acetylation was detected for GST-K24R/K43R-(1–189) and GST-K24A/K43A-(1–189) (Fig. 4*C*), which is consistent with the results of the *in vivo* acetylation assays. Autoacetylated p300-HAT was observed in the very top in all lanes except the one without p300-HAT. To preclude the possibility that substitution of Lys-24 and Lys-43 can disrupt the interaction between AML1 and p300, we performed immunoprecipitation experiments by transiently expressing p300 with AML1 and K24A/K43A in 293T cells. The mutant formed a complex with p300 as effi-

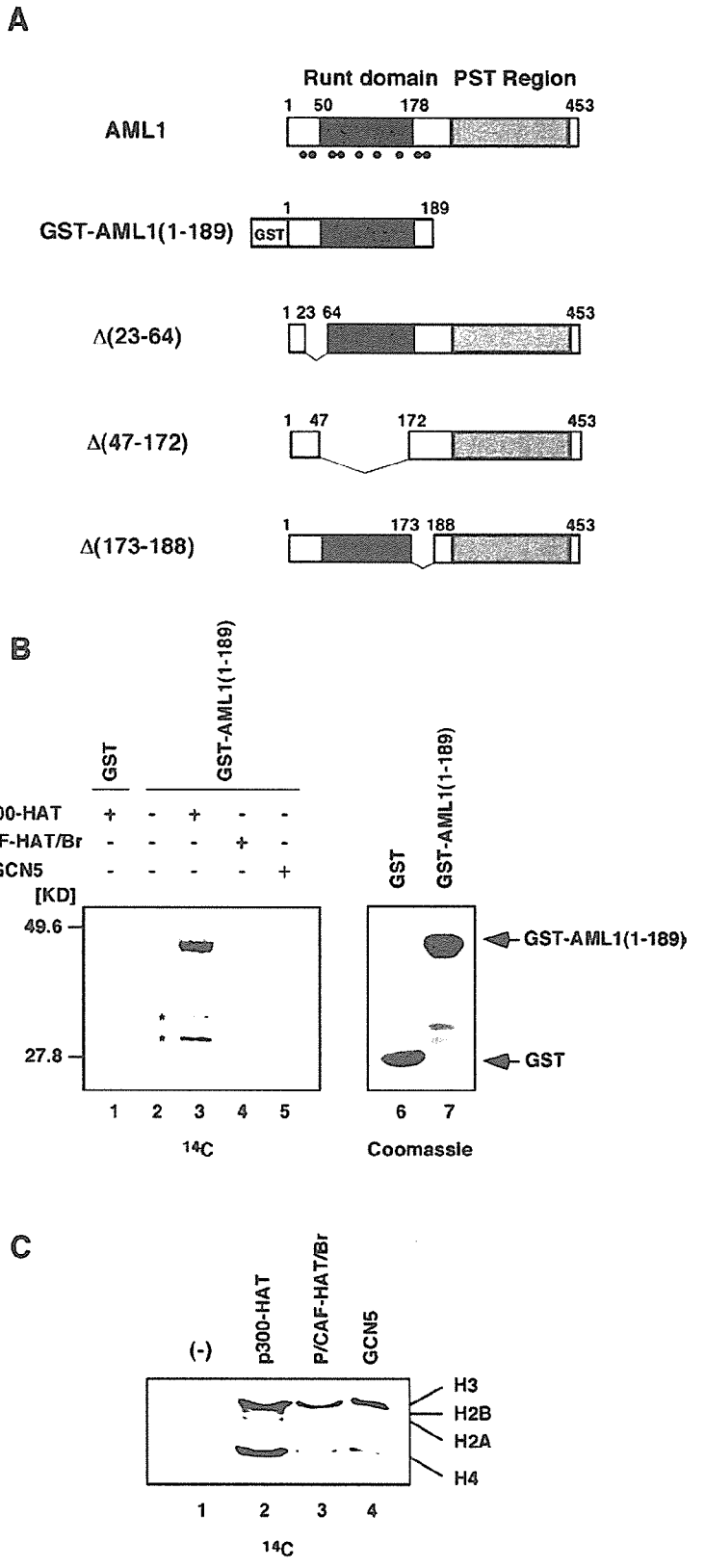

FIG. 2. ***In vitro* acetylation of AML1 by p300-HAT.** *A*, structures of AML1 and GST-AML1 fusion constructs used as substrates for p300. The Runt domain is *closed*. The PST region and GST are *shaded*. The positions of lysine residues are indicated by the *closed circles*. *B*, the *in vitro* acetylation assay of AML1 with p300-HAT, P/CAF-HAT/Br, and GCN5. Purified GST or GST-AML1-(1–189) protein was incubated with or without each recombinant HAT in the presence of [^{14}C]acetyl-CoA for 1 h at 30 °C. Reaction products were resolved by SDS-PAGE (*lanes 1–5*). The gel was stained with Coomassie Blue to demonstrate that the equivalent substrate was used in each reaction (*lanes 6* and *7*). *Asterisks* indicate degraded products of acetylated AML1. *C*, histone acetylation by various HATs. Histones (H2A, H2B, H3, and H4) were incubated either with or without each recombinant HAT in the presence of [^{14}C]acetyl-CoA for 1 h at 30 °C followed SDS-PAGE as described above.

ciently as wild type AML1 in 293T cells (data not shown). These results imply that loss of acetylation in the Lys-24/Lys-43 mutant does not result from their inability to associate with p300 but suggest that these two lysines are authentic targets for acetylation by p300.

Acetylation Augments Site-specific DNA Binding of AML1—Having identified an AML1 mutant that cannot be acetylated by p300, we set out to use this mutant to dissect the functional consequence of AML1 acetylation. For a growing number of transcription factors, it has been suggested that acetylation

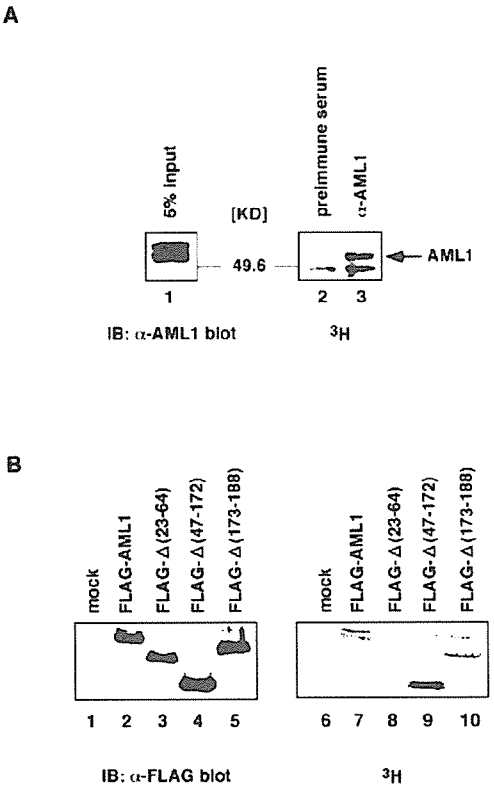

FIG. 3. **Acetylation of AML1 *in vivo*.** *A*, lysates from MOLT-4 cells pulse-labeled with 1 mCi of sodium ^{3}H/ml in the presence of 50 nM trichostatin A were immunoprecipitated with anti-AML1 or preimmune serum as a control. Immunoprecipitated samples were resolved by SDS-PAGE. Proteins were electrotransferred onto polyvinylidene difluoride membrane and immunoblotted (*IB*) with anti-AML1 (*lane 1*) or analyzed using BAS2000 image analyzer (*lanes 2* and *3*). Input represents 5% of the radiolabeled protein used in the assay. Locations of molecular mass markers and AML1 are shown. *B*, COS7 cells were transfected with 10 μg of pME18S, FLAG-tagged wild type AML1, or the FLAG-tagged deletion mutants of AML1, together with pcDEF3-p300 as indicated, and were labeled with sodium [^{3}H]acetate in the presence of trichostatin A. Whole cell lysates were immunoprecipitated with anti-PST and subsequently resolved on SDS-PAGE (*right*). Expression of each protein is monitored by immunoblotting of whole cell lysates with anti-FLAG (*left*). *mock*, mock-infected.

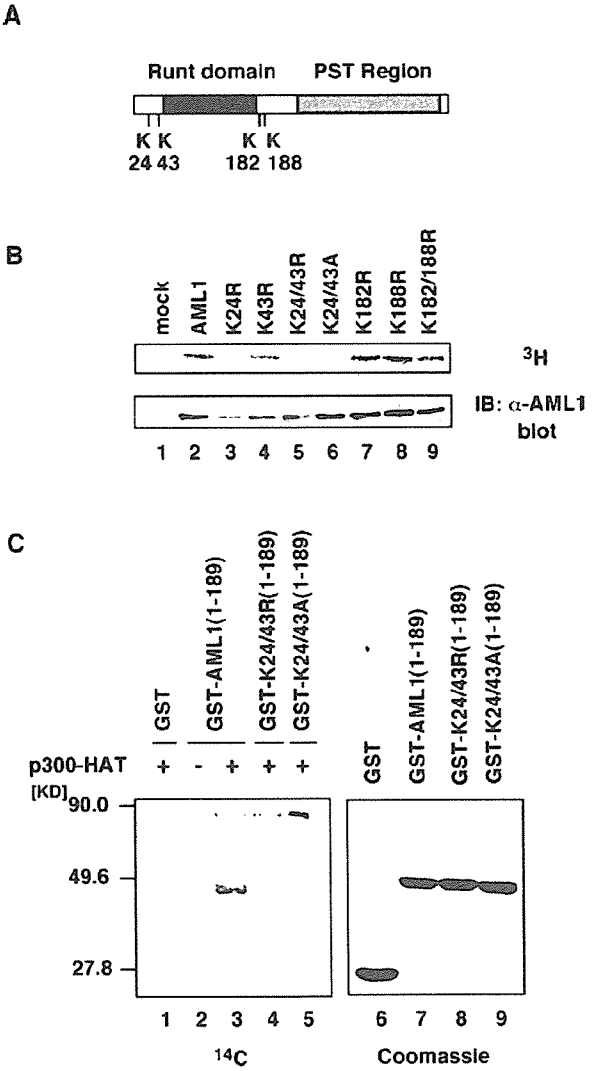

FIG. 4. **Determination of lysine residues acetylated by p300.** *A*, positions of lysine residues outside the Runt domain. *B*, the lysine mutants of AML1 were transfected into COS7 cells together with pcDEF3-p300. Transfected cells were pulse-labeled with sodium [^{3}H]acetate for 90 min. Whole cell lysates were immunoprecipitated with anti-PST and resolved by SDS-PAGE (*top*). The expression levels of each construct were monitored by immunoblotting (*IB*) of whole cell lysates with anti-AML1 (*bottom*). *mock*, mock-infected. *C*, GST fusion proteins were incubated with or without purified FLAG-tagged p300-HAT in the presence of [^{14}C]acetyl-CoA, as indicated. Reaction mixtures were separated by SDS-PAGE, fixed, and stained with Coomassie Blue (*lanes 6–9*). The stained gel was dried, and ^{14}C incorporation was visualized by BAS2000 image analyzer (*lanes 1–5*).

plays a key role in the regulation of sequence-specific DNA binding (40, 42). Since acetylation can lead to a change in the charge and the size of the lysine residues (53), it is likely that acetylation impinges on the affinity of AML1 for DNA. To test this possibility, electrophoretic mobility shift assays were performed with purified proteins for GST-AML1-(1–189) or its lysine mutant, both of which possess the Runt domain that is responsible for binding to the PEBP2 site (11, 12). Each protein was incubated with bacterially produced p300-HAT and radiolabeled M4 probe, double-stranded oligonucleotide bearing the PEBP2 site, and DNA binding abilities were evaluated. When M4 probe was incubated with GST-AML1-(1–189) and p300-HAT in the absence of acetyl-CoA, we observed a shifted band that was not seen for GST (Fig. 5*A*, *left*). The shifted band was significantly reduced when an excess of the cold probe was added, indicating that the AML1-DNA complex was formed through specific binding of AML1 to the PEBP2 sequence. We then determined the effect of p300-mediated acetylation on DNA binding of AML1. The addition of acetyl-CoA greatly augmented the shifted band (Fig. 5*A*, *left*, *lane 4*), indicating DNA binding of AML1 specifically enhanced by acetylation. In contrast, K24R/K43R substitution in GST-AML1-(1–189) significantly abolished the DNA binding ability of AML1, and no increase in DNA binding was found even upon the treatment of acetyl-CoA (Fig. 5*A*, *left*, *lanes 5* and *6*). Coomassie staining of each recombinant protein indicated the presence of equal amounts of the GST-AML1 proteins (Fig. 5*A*, *right*).

Because PEBP2β is a key regulator for DNA binding of AML1, we next tested the effect of AML1 acetylation on DNA binding in the presence of PEBP2β. As shown in Fig. 5*B* (*left*), GST-AML1-(1–189) in the presence of bacterially produced PEBP2β showed a sequence-specific DNA-binding complex that was markedly diminished by the addition of the cold probe. K24A/K43A mutation abolished the DNA binding ability of AML1 even in the presence of PEBP2β (Fig. 5*B*, *left*). The K24R/K43R mutant, which maintains the positive charge also exhibited severely impaired DNA binding, indicating that al-

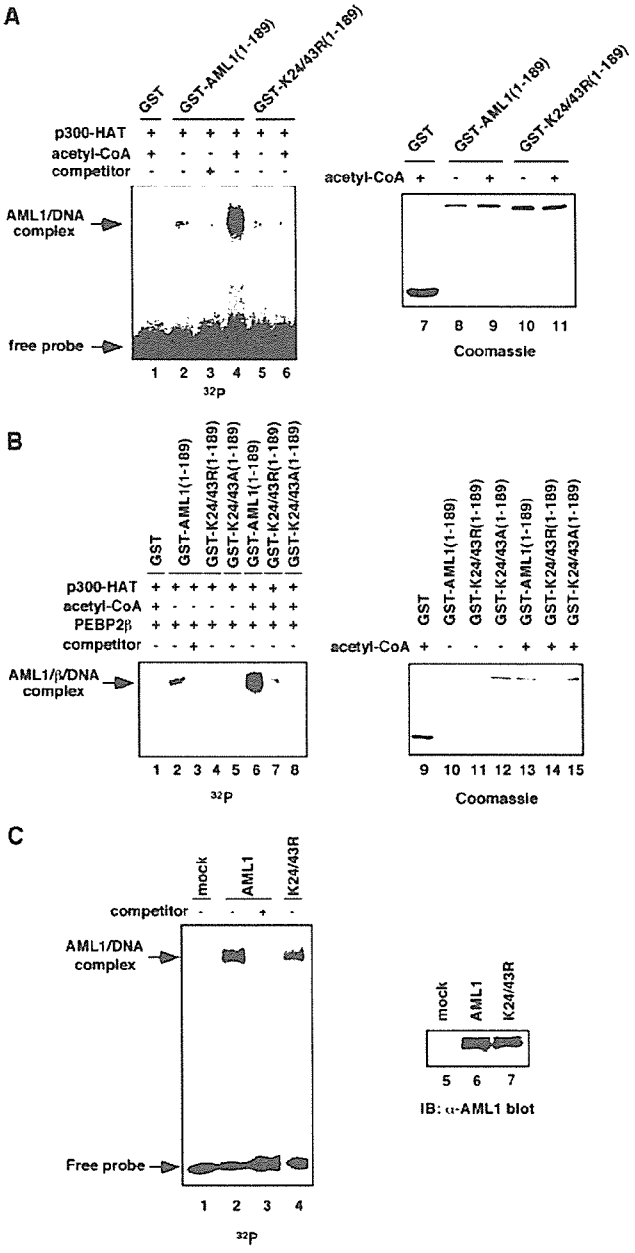

FIG. 5. **The DNA binding activity of AML1 is augmented by acetylation.** *A*, EMSAs demonstrating DNA binding of acetylated and unmodified AML1. Purified GST, GST-AML1-(1–189), or its lysine mutant (GST-K24R/K43R-(1–189)) was incubated with p300-HAT and the ^{32}P-labeled M4 probe either in the presence or in the absence of acetyl-CoA, as indicated (*left*). Excess of the unlabeled M4 probe was used as a competitor. Amounts of purified GST fusion proteins used in EMSA were monitored by Coomassie staining (*right*). *B*, DNA binding of unmodified (*lanes 2–5*) and *in vitro* acetylated GST, GST-AML1-(1–189), or its lysine mutant (GST-K24R/K43R or A-(1–189)) (*lanes 6–8*) was tested by EMSA as indicated above in the presence of bacterially expressed and purified PEBP2β (*left*). Coomassie staining exhibits the equal amounts of GST fusion proteins used in EMSA (*right*). *C*, the ^{32}P-labeled M4 probe was co-incubated with nuclear extracts (containing 18 μg of proteins) from COS7 cells co-transfected with the control vector, the wild type of full-length AML, or K24R/K43R together with PEBP2β (*left*). Expression of each protein was monitored (*right*). *IB*, immunoblot.

tered DNA binding results from a block of acetylation of Lys-24/Lys-43 rather than a fundamental change in the conformation of the mutants. Impaired DNA binding in these mutants was not restored by the addition of acetyl-CoA, which significantly enhanced DNA binding of the AML1-PEBP2β complex. Coomassie staining of each recombinant protein indicated the presence of equal amounts of the GST-AML1 proteins (Fig. 5*B*, *right*). These results indicate that PEBP2β cannot fully overcome a decrease in DNA binding of the AML1 mutants defective for acetylation.

To obtain further evidence that acetylation of target lysines alters DNA binding of AML1, we examined the effect of acetylation on sequence-specific DNA binding using full-length AML1 and its arginine mutant (K24R/K43R) in the presence of PEBP2β. We performed EMSA with nuclear extracts of COS7 cells transfected with mock, full-length AML1, and K24R/K43R together with PEBP2β. When the M4 probe was incubated and electrophoresed with nuclear extracts containing wild type AML1 in the presence of PEBP2β, a distinct band was observed that was not recognized in the lane loaded with the mock transfectant (Fig. 5*C*, *left*, *lanes 1* and *2*). This band became undetectable when a cold probe was coincubated with a labeled probe (*lane 3*), indicating that it represents a specific AML1-DNA complex. We again found that DNA binding of K24R/K43R was significantly reduced, although it still remained at a detectable level. Immunoblot analysis of nuclear extracts confirmed the presence of equal amounts of the AML1 proteins in all samples (Fig. 5*C*, *right*). Taken as a whole, these results demonstrated that DNA binding of AML1 could be regulated by acetylation of Lys-24 and Lys-43.

Heterodimerization with PEBP2β Is Not Modulated by Acetylation of AML1—The affinity of AML1 for DNA is markedly increased by heterodimerization through the Runt domain with PEBP2β, which could not interact with DNA by itself (10–13). It is possible that the altered interaction with PEBP2β could determine the DNA binding property of acetylated AML1. We asked, therefore, whether mutation of Lys-24 and Lys-43 in AML1 affects the interaction with PEBP2β. COS7 cells were transfected with wild type AML1, K24R/K43R, or K24A/K43A together with PEBP2β. The cells were lysed and immunoprecipitated with anti-PST and then subjected to immunoblot analysis using anti-PEBP2β. As shown in Fig. 6*A*, K24R/K43R and K24A/K43A associated with PEBP2β as effectively as wild type AML1. The expression level of each construct was confirmed by immunoblotting of whole cell lysates. These data indicate that Lys-24 and Lys-43, the target residues for acetylation, are dispensable for heterodimerization between AML1 and PEBP2β, suggesting that acetylation of AML1 does not affect the affinity for PEBP2β.

Acetylation by p300 Stimulates Transcriptional Activation of AML1—Because DNA binding of AML1 is stimulated in an acetylation-dependent manner, it is tempting to speculate that the transcriptional activity of AML1 can potentially be regulated by acetylation. To determine this, we examined whether substitution of Lys-24 and Lys-43 could modify transcriptional responses induced by AML1. For these experiments, we employed a reporter plasmid pM-CSF-R-luc in which the M-CSF receptor promoter is linked to the luciferase gene because it is efficiently activated by exogenous expression of AML1 (29). Wild type AML1, K24R/K43R, or K24A/K43A was introduced into HeLa cells, which lack endogenous AML1 activity, together with the reporter plasmid, and then luciferase activities were evaluated. As shown in Fig. 6*B*, we observed a 7-fold activation of pM-CSF-R-luc when wild type AML1 was expressed. In contrast, both K24R/K43R and K24A/K43A showed a significantly reduced transcriptional activation. Although p300 expression further enhanced the transcriptional activity of wild type AML1, impaired transcription by K24R/K43R and K24A/K43A was not restored even in the presence of p300. We confirmed that both K24R/K43R and K24A/K43A were ex-

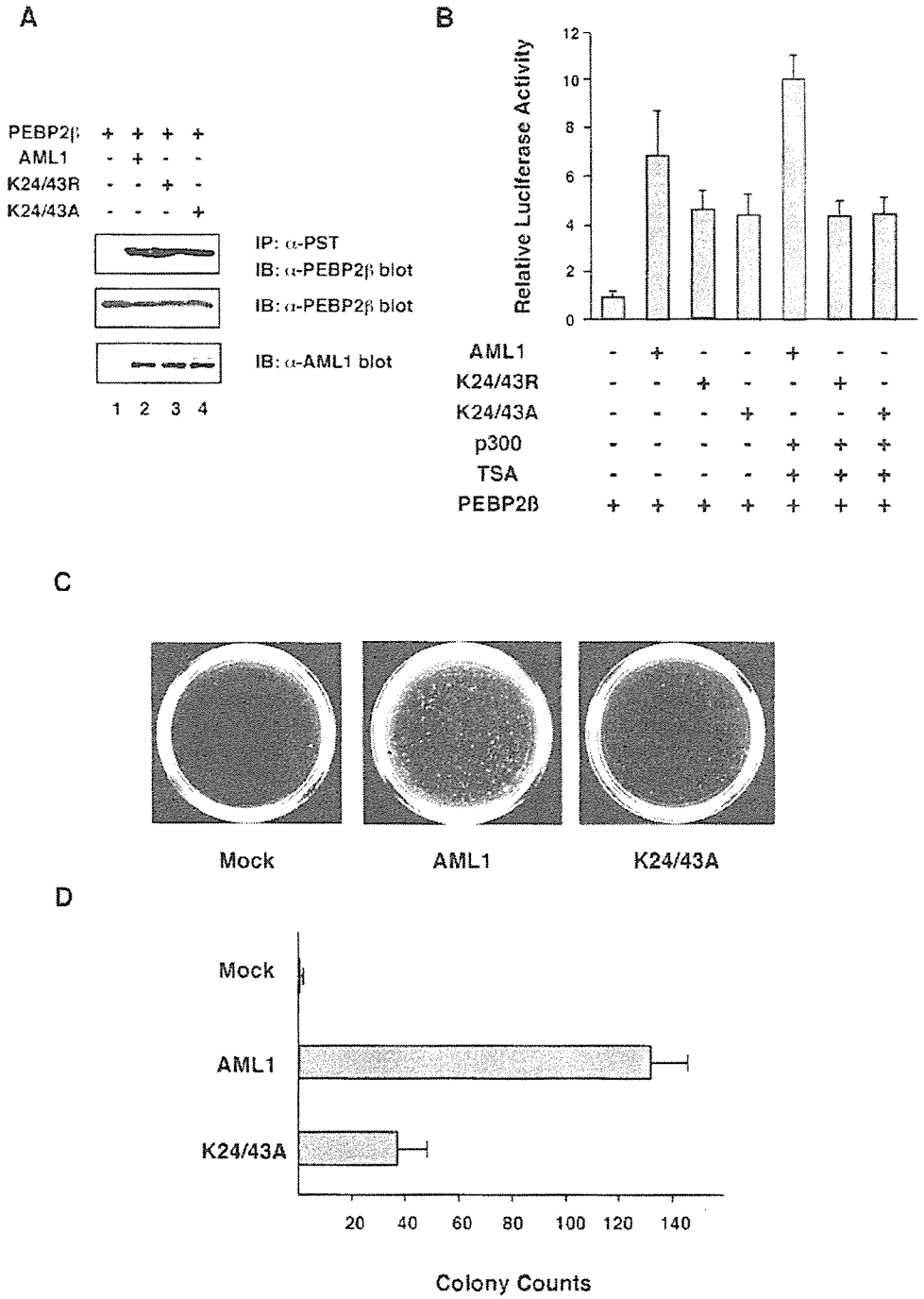

FIG. 6. *A*, interactions of wild type and the lysine mutant of AML1 with PEBP2β. COS7 cells were transfected with pME18S, wild type AML1, K24R/K43R, or K24A/K43A, together with PEBP2β as indicated. Cells were lysed, immunoprecipitated (*IP*) with anti-PST, and subjected to immunoblotting (*IB*) with anti-PEBP2β (*top*). Expression of each protein is monitored by immunoblotting of whole cell lysates with either anti-PEBP2β or anti-AML1 (*middle* and *bottom*). *B*, acetylation of AML1 stimulates its transcriptional activity. pM-CSF-R-luc was co-transfected into HeLa cells with each set of expression plasmids either with or without co-expression of p300, and the cells were analyzed for luciferase activity. Trichostatin A was added where indicated to a final concentration of 50 ng/ml at 8 h prior to harvest. Values of the relative luciferase activity and *error bars* represent the means and the standard deviations, respectively, for three independent experiments. *C*, soft agar assays with NIH3T3 cells expressing AML1 and the K24A/K43A mutant. NIH3T3 cells infected with retroviruses for AML1 or K24A/K43A of a comparable titer were seeded in soft agar after G418 selection and cultured for 14 days. Cells infected with AML1 gave larger average colony sizes and increased colony numbers, whereas cells infected with K24A/K43A created barely macroscopic colonies in agar as well as mock-infected (*mock*) cells. *D*, comparison of transforming activities of AML1 and K24A/K43A. Colonies greater than 0.25 mm in diameter were counted as positive. *Numbers* and *error bars* show the means and standard deviations of colony counts, respectively, for three independent experiments.

pressed as efficiently as wild type AML1 in HeLa cells (data not shown). These data strongly suggest that p300-mediated acetylation of AML1 on Lys-24 and Lys-43 is required for the optimal transcriptional activation of AML1.

Disruption of the Target Lysines Impairs Fibroblast-transforming Activity of AML1—Previously, we reported that overexpression of AML1 induces neoplastic transformation of NIH3T3 cells depending on the DNA binding ability and the